Mineralization and sustainable development in West African Craton: From field observations to modelling

Tahar Aïfa

Accepted Manuscript

Geological Society, London, Special Publications

Mineralization and sustainable development in West African Craton: From field observations to modelling

Tahar Aïfa

DOI: https://doi.org/10.1144/SP502-2021-21

To access the most recent version of this article, please click the DOI URL in the line above. When citing this article please include the above DOI.

Received 27 January 2021
Revised 19 March 2021
Accepted 19 March 2021

Mineralization and sustainable development in West African Craton: From field observations to modelling

Tahar Aïfa

Univ Rennes, CNRS Geosciences Rennes - UMR 6118, F- 35000 Rennes, France

Abstract

This Special Publication combines results obtained by interdisciplinary groups from numerous academic institutions working on Paleoproterozoic formations to decipher the origins of the main mineralization resources in the West African Craton (WAC) and their impacts on African economic development. Structural, geophysical, sedimentological, stratigraphical, geochemical, petrophysical and mineralogical analyses have been used to highlight the complexities involved in mineralization emplacement and its origin and evolution within the WAC. Fourteen articles, mainly of basic research carried out in the WAC and surrounding areas, contribute to new knowledge in mineral research with updated references. They show that the geodynamic evolution of the WAC is complex from one area to another: it involves subduction, collision and obduction during several deformation phases ranging from Birimian (2.3-2.0 Ga) to Pan-African (650-450 Ma) events. Mineralization is mainly controlled by tectonics within shear zones, orogenic belts, basins and faulting systems occurring in the various corridors. Mineralized fluid circulation is stressed and injected into appropriate formations and precipitate several types of well-documented ore deposits: porphyry, metal-bearing, volcanogenic massive sulfide, sedimentary exhalative and lateritic. Various modelling techniques, when integrated help to understand the mechanisms of mineralization emplacement, some of which are still a matter of debate. Traditional and industrial exploitation of ore deposits, mainly gold, may inadvertently cause pollution to water tables and rivers, thus affecting the environment including watersheds. The challenge for further studies is mitigation for sustainable development that can be appropriately used to minimize such damage.
The aim of this volume is thus to bring new insights to research activities on ore deposits within the WAC.

Keywords : *Mineralization, West African Craton, Geodynamics, ore deposit, exploration, modelling*

Introduction

Several special books have been devoted to research on mineralization, ore deposits, some of which focused on modelling and emplacement mechanisms of valuable minerals/ores within rocks. However, new specifications have made it possible to enforce limits on the impact of mining on the environment and the health of civil populations by the mining industry. Not only have they contributed through financial support to the economy of the developing countries but also in the mitigation and remediation of mines during and after their exploitation and their impact on the environment, health, employment, etc. (e..g. Pokorny et al., 2019).
Many meetings resulted in proceedings or special books on the geology and mineral deposits of the WAC, such as the International Geoscience Programme IGCP 485 (2003-2007, Cratons, metacratons and mobile belts: Keys from the West African craton boundaries, Eburnian versus Pan-African signature, magmatic, tectonic and metallogenic implications), IGCP 502 (2004-2008, Global comparison of volcanic-hosted massive sulfide districts: the controls on distribution and timing of VMS deposits) and Workshops including a meeting on the Geology and Metallogenesis of the Hoggar and Eglab massifs held in Tamanrasset (Algeria) on March 1-3, 2005. Most of the meetings were followed by a field trip to highlight outcrops that contain ore deposits. This volume presents a series of articles dealing with ore deposit investigations in the WAC and surrounding areas. This collection

of fourteen research papers arose as the result of keynote presentations, guests and volunteers given mainly at the 4th meeting of the IGCP project 638 (2016-2021, Paleoproterozoic Birimian Geology for Sustainable development).

A significant number of papers related to the geology of the WAC have been published, as summarized by Van Hinsbergen et al. (2011) in a previous special book on the formations of Africa (from 3.8 Ga to present). But papers focusing on WAC mining research are limited (e.g., Aïfa, 2008, 2018 ; Saddiqi et al., 2018).

In this special publication, the focus is on the WAC and its surrounding areas, dedicated mainly to ore deposits from exploration using various tools (geophysics, geochemistry, petrology, sedimentology, etc.) to the implementation of modelling work through the application of recent exploration techniques and ore identification (Fig. 1a,b).

An attempt to correlate the WAC with other terranes/plates (Rio de La Plata, Baltica, etc.) since the Archean regarding mineralization areas has also been made (e.g., Onstott et al., 1984; Franceschinis et al. 2019, Masquelin et al., 2021). They indicate that most of the areas where mineralization occurs are linked or occupy the boundary between terranes (large-scale shear zones) (e.g., Diène et al., 2015; Masurel et al., 2017). As noted in a simplified sketch (Fig. 2), at such boundaries, along with subducting plates or along ridges, significant mineral deposits are often developed. Some studies have focused on the relationship with alteration/mineralization within the WAC formations (e.g., Ben Aissi et al., 2005; Fon et al., 2012; Giorgis et al., 2014; Siagné et al., 2021).

Ore deposit focused research activity is increasing nowadays due to the recent demand for metallic ore in different fields, mainly electronics, health, industry and agriculture and owing to rising prices of certain metals such as PGE (e.g., Maier, 2005; Augé et al., 2012). The use of modern investigative tools in the field as well as in the laboratory has greatly improved the understanding of the mechanisms of ore deposits and their interpretation, since the areas of research for such investigations concern a field as wide as sedimentology, stratigraphy, metamorphic petrology, tectonics, structural geology, geochemistry, geochronology, metallogenesis, gravity and magnetism, seismic, GIS, remote sensing, etc (e.g., Chapman et al., 2002; Mickus, 2008; Johnson et al., 2013; Yousefi and Nykänen, 2017). This volume will be of interest to all those involved in mining research or exploration concerned with the above investigative tools. Several special issues have been published in the past suggesting a great interest in the timing of the formation of metal ore deposits (e.g., Franklin, 1996; Sangster, 1996b; Blundell et al., 2002; Ennih et al., 2004; Aïfa, 2008, 2018 ; Ennih and Liégeois, 2008; Belkasmi and Ennih, 2010; Driouch et al., 2010; Jessell and Liégeois, 2015; Jessell et al., 2016; Saddiqi et al., 2018).

Ore deposits provide new evidence for magmatism associated with cratons or metacratons and their boundaries where major fractures or shear zones exist, through which fluid circulations and alterations may occur (e.g., Johnson et al., 2013). Hydrothermal fluids can be the source of mineralization such as oxides, sulfides, gold or PGE ore deposits (e.g. Milési et al., 2006; Jefferson and Delaney, 2007; Tshibubudze and Hein, 2013). What controls the genesis of ore deposits in ‘‘stable” areas like the WAC and what are the geodynamic and the metamorphic processes that lead to the formation of ore deposits? Several issues have been addressed to help the reader understand the genesis of the ore deposits, their evolution and how they may be extracted (see e.g. Cook and Marshall, 2004; McLaurin et al., 2005; Els and Eriksson, 2006; Zaw et al., 2007; Chapman et al., 2009, 2017).

The papers presented in this volume include results from large-scale field exploration and presenting vast amounts of new data using techniques based on various processing methods.

Based on geodynamic models linked to the African cratonic lithosphere, one can distinguish areas with different Archean lithosphere thicknesses, in particular within the WAC, revealed by seismic tomography (Celli et al., 2020). However, several models of mineralization of ore deposits (e.g., McQueen, 2005), with their own emplacement mechanisms, are sub-divided into five main types (i to v):

(i) Production of different types of deposits: porphyry copper, sulfur, gold-silver by infills of veins, but also lead-zinc veins (Fig. 3a). Most of Africa's copper production comes from the Central African Copper Belt. However, the WAC copper mines are located in its northwestern limit or in the north Atlas range. Porphyritic copper deposits form beneath stratovolcanoes (Fig. 3a) where copper can be concentrated in hot, salty hydrothermal fluids in the molten igneous rock of the volcano. Copper settles as the molten rock cools and solidifies and/or is expelled with the hydrothermal fluids and deposit into adjacent rocks as the fluids cool and release their metallic charge. An average porphyritic copper deposit may contain 140 Mt of ore and consists of 0.5% copper (Singer et al., 2002).

(ii) Presence of metal-bearing: it requires magmatic intrusions such as the example of the Sampleu mafic–ultramafic intrusion in western Côte d'Ivoire (e.g., **Gouedji et al., 2020**) (Fig. 3b). Zinc and lead are commonly found in ore deposits that form from hydrothermal fluids at low-temperatures. Several types of deposits are recognized based on how the hydrothermal fluids were generated and their movement, the distribution of minerals in the deposit, and the geological context. Two deposit types formed on or near the ancient ocean floor where hydrothermal fluids moved to the seabed along fractures and vented to form hot springs (Fig. 3b).

(iii) Volcanogenic Massive Sulfide (VMS) deposits: classified as hydrothermal deposits, many of which are associated with magmas generated at convergent plates boundaries such as porphyry copper (type i) deposits. VMS deposits are associated with the eruption of volcanic rocks underwater. Indeed, deposits form where the magma cools, either on the ocean floor or emplace at depth in shallow intrusions, providing the heat necessary to generate and mobilize hydrothermal solutions (Lydon, 1988; Franklin, 1993, 1996; El Basbas et al., 2020). The oldest (Archean) VMS deposits have been reported to contain less lead than younger ones (e.g., Meso-Cenozoic). They can also contain recoverable amounts of copper, gold, and silver. They are a common deposit type but are currently not important for metal production in the WAC (Belkabir et al., 2008; Marcoux et al., 2008; Moreno et al., 2008; **Outigua et al., 2020**) (Fig. 3c). However, hydrothermal solutions mixed with seawater and deposited amounts of iron, zinc, and lead on the mounds and layers of the seabed can thus form a VMS-type deposit (Fig. 3c).

(iv) Sedimentary exhalative (sedex) deposits: they concern the hydrothermal solutions, generated as water-rich sediments, buried deep in basins, then expelled when pressure is released during folding and faulting (Goodfellow et al., 1993; Lydon, 1996; Kolb and Petrov, 2016) (Fig. 3d). Sedex lead and zinc deposits are a type of hydrothermal deposit found in sedimentary basins. These basins generally form when the continents are rifted apart. Sedex deposits are typically found in large basins filled with more than 10 km of sediment. Silver, and less commonly copper, can be present in economical quantities in sedex deposits. Globally, sedex deposits are younger than 1800 Ma. Examples of sedex deposits in Africa relate to lead-zinc deposits that form from hydrothermal fluids associated with sedimentary basins. However, in these deposits, hydrothermal fluids move through aquifers, mix with other fluids, and deposit minerals in open cavities within carbonate sedimentary rocks such as limestone. These ore bodies are referred to as Mississippi Valley type (MVT) (Sangster, 1996a,b; Leach et al., 2005, Haldar, 2020). The movement of hydrothermal fluids in the sedimentary basins is driven by forces resulting from interactions at the plates boundaries. These deposits form in relatively undeformed sedimentary rocks that generally occur inland from the mountain belts formed at convergent plate margins (Fig. 2). Known MVT deposits are younger than 500 Ma. Jurassic carbonate

rocks of the High Atlas Mountains in northeastern Morocco and in northern Algeria (Fig. 1b) host the largest known MVT deposits in Africa (Bouabdellah et al., 1999).

(v) *Soil profile and alteration*: it is related to alteration soil which may have produced either iron (Mauritania, Algeria, etc.) or bauxite (Burkina-Faso, Côte d'Ivoire, etc.) (e.g., Ciampalini et al., 2013 ; Giorgis et al., 2014; Metelka et al., 2015, 2018). In fact, e.g., bauxite is formed by weathering of aluminium-bearing rocks in high relief terrain and good drainage in tropical climate (e.g., alternating wet and dry seasons). A similar process can be given for iron (Fig. 3e). Most nickel and cobalt come from two general types of deposits: nickel laterite and igneous (magmatic) nickel-sulfide deposits. Nickel laterite (Fig. 3e) is formed by the weathering of nickel-bearing rock in areas with a tropical climate and good drainage (Freyssinet et al., 2005). During this process, silica and other components are leached from the rocks, leaving a soil enriched in nickel, cobalt, and iron. The main nickel minerals are garnierite (hydrous nickel silicate) and nickeliferous limonite (hydrated nickel-bearing iron oxide). Igneous (magmatic) nickel-sulfide deposits are associated with igneous rocks rich in magnesium, nickel, and chromium. These mafic and ultramafic rocks form as magmas cool and crystallize in layered igneous complexes. Then, a separate liquid, rich in sulfur, iron, nickel, copper, and occasionally PGE can form within the magma. The sulfur-rich liquid, which is denser than the silicate-rich magma, will not mix again with the silicate-rich magma. Eventually, liquids rich in sulfur-iron nickel-copper separately accumulate and solidify to form a variety of minerals that include pentlandite (iron nickel sulfide), which is mined for its high nickel content (Naldrett, 2004; Arndt et al., 2005). Nickel laterite deposits are present throughout equatorial Africa, wherever tropical climatic conditions and nickel-rich rocks coexist. The most significant nickel laterite deposits are located in Burundi, and in Côte d'Ivoire (Hammerbeck and Schurmann, 1998).

West African countries have experienced the highest levels of exploration activity for the past two decades, particularly in Mali, Ghana, Burkina Faso and Côte d'Ivoire (Wilburn, 2004). Unlike the other parts of Africa where lode/vein gold deposits are associated mainly with rock units formed prior to 2.5 Ga, the major source of gold in the WAC has been rock units formed between 2.5 and 1.6 Ga. These younger rock units and related structures trend north to northeast and underlie much of western Ghana, Côte d'Ivoire, and Burkina Faso, and extend into the western part of Nigeria and southern Mali (Fig. 1a). It is in these areas that many of the recent important gold discoveries have been made and that are most prospective for new discoveries. Among the five ore deposit types, i.e., (i) porphyry, (ii) metal-bearing, (iii) volcanogenic massive sulfide, (iv) sedimentary exhalative and (v) lateritic, many regions in the WAC have been subjected to deep weathering, and the potential for lateritic nickel deposits is being recognized, such as those known, e.g., in Côte d'Ivoire. The Biankouma-Touba deposit in Côte d'Ivoire (Fig. 1b) has a resource of 169 Mt at 1.77% nickel and 0.08% cobalt, but requires massive investment since it is far from railway and harbor facilities. The primary nickel (sulfide) deposits in the WAC are mostly associated within magnesium-rich intrusive rocks (ultramafic rocks). Whereas the diamond potential of the central part of the WAC, buried beneath the sands of the Sahara, is still to be evaluated. Recent exploration in Mauritania (Reguibat Shield) and Algeria (Yetti-Eglab Shield and Reggane Basin) has found commercial-size diamonds and G10 pyrope garnets (larger than 1 mm) and work continues to locate the kimberlite source rocks (Allek and Hamoudi, 2008 ; Kahoui et al., 2008 ; Markwitz et al., 2016).

Section 1: Minerals and mineralization

(1) The article of **Aït Hmeid et al. (2020)** concerns the Ibourhardayn bentonite clay deposit of Beni Bou Ifrour within the Gourougou volcanic massif, in northeastern Morocco, in terms of mineralogical, chemical and geotechnical characteristics (e.g., Al-Juboury, 2018). This massif is mainly composed of sedimentary, volcanic and granodioritic rocks from the Mesozoic to the Neogene (El Rhazi and Hayashi, 2002). The Iburhardayn deposit results from the weathering of volcanic ash and brecciated pyroclastic flows which have typical transport characteristics (Ddani et al., 2005). It consists of two significant bentonite layers: lower and upper layers resting on (i) Miocene marls covered by trachyandesite tuffs, on top of which (ii) a thin volcanic ash (cineritic) facies occurs, respectively. They are hosted in a sandy marl basement with biodetritic levels containing algae and bryozoans. Fossil fauna and flora are typical of shallow marine waters for lagoon lacustrine environments (Asebriy and Cherkaoui, 1995; Ddani et al., 2005).

After a quick review of the bentonite deposits over the world and detailed chemical description of the bentonites, the authors used some useful characteristics for sustainability as good candidates for pollutant adsorbents. Experimental analysis on the bentonite was performed to extract its physico-chemical and mineralogical compositions and its textural properties using X-ray diffraction, particle size distribution, sedigraphy, bulk density, liquid limit, plastic limit and shrinkage limit.

The Ibourhardayn materials are of Ca-bentonite type (Inglethorpe et al., 1993; Zeng et al., 2019). The differences in the plasticity of the samples analyzed are due to the variation in grain size distribution and to mineralogical composition, i.e. samples with high clay content have a high plasticity, whereas the silt fraction is characterized by relatively low plasticity. They also show that this bentonite represents a mixture of montmorillonite, anorthite, albite and orthoclase feldspar, with some calcite and impurities. Additionally, it has a very high water retention capacity and therefore a high swelling capacity, similar to some other bentonite outcrops (Ben Hamouda et al., 2017).

(2) In their paper on the Bou Azzer inlier, **Ikenne et al. (2020)** carried out a synthesis on the cobalt-nickel-copper (Co-Ni-Cu) deposits at Bou Azzer (Anti-Atlas, Morocco). In this well-known mining area, mineralization, associated with large bodies of serpentinite, results from alteration of Neoproterozoic ophiolite sequences including peridotite protoliths through Pan-African Orogeny (800-540 Ma). These ophiolites were subject to (i) a major tectonic lineament, the Anti-Atlas Major Fault (AAMF; Leblanc, 1981; El Boukhari et al., 1992; Saquaque et al., 1992) and (ii) tectono-magmatic events of Pan-African, Hercynian and Alpine ages, at the origin of the polyphase history of the Anti-Atlas (Choubert, 1952; Leblanc, 1981; Hassenforder, 1987). They induced progressive enrichment in Co and Ni mineralization with the primary mineralization and its remobilization (Leblanc, 1981; Maacha et al., 1998; Maacha, 2013). In this work, the authors try to demonstrate, after a review of general and local geology [Precambrian lithostratigraphy and geodynamics of the Anti-Atlas through Pan-African Orogeny], how mineralization can be controlled by tectonics (faults, lithology) and constrained by mineral paragenesis and mineral chemistry. However, the lithostratigraphy of the Bou Azzer inlier has been recently refined (Chèvremont et al., 2013; Blein et al., 2014).

The 2500 m thick pile of ophiolitic sequence is composed of mafic and ultramafic rocks and a dyke complex associated with a volcanosedimentary sequence, including pillow-lavas and pyroclastic flows (Leblanc, 1981). The ultramafic rocks underwent serpentinization, including disseminated and podiform chromites (Ikenne et al., 2005; Ahmed et al., 2009; Hodel et al., 2017). It occurred through (i) oceanic-like serpentinization at temperatures of 350-200°C of fresh serpentinites, followed by (ii) a hydrothermal event involving Cl-rich acidic fluids that significantly altered them. The calc-alkaline geochemistry of the mafic rocks and the chemistry of chromitic minerals are compatible with a suprasubduction arc setting (Bodinier et al., 1984; Ikenne et al., 2005; Ahmed et al., 2009).

A genetic model for the Bou Azzer deposits has been proposed through the timing of mineralization and the source(s) of metals for this odd mineralized system. It can be explained through two main arguments (i) occurrence of possible discrete events of polyphase mineralization/remobilization, and (ii) identification of the source(s) of metals and arsenic. The following conclusions were thus drawn (Maacha et al., 1998), complemented by stable isotope geochemistry (Levresse, 2001 ; Dolansky, 2007 ; Maacha, 2013): (1) A primary stage of Co-Ni arsenide-sulfarsenide mineralization, hosted within an E-W, ENE Pan-African faulting system (~615 Ma) ; (2) accompanied by extensional deformation at the onset of basin opening in the early Ediacaran ; (3) reactivated during the Pan-African compressive tectonics starting from c. 615 Ma ; (4) A second mineralization stage (Maacha et al., 1998, 2015) during extensional tectonics at the Ediacaran-Cambrian transition ; (5) Extensional tectonics would have favored upward movement of serpentinite domes through the reactivation of the mineralized faulting system ; (6) High salinity basinal brines with high chloride content (Leblanc and Lbouabi 1988; En-Naciri, 1995; En-Naciri et al., 1995; Lebedev et al., 1999; Essaraj et al., 2005; Dolansky, 2007), leaching and mobilizing of metals (e.g. Co, Ni), possibly from serpentinites. The mixing of such a fluid with a serpentinite-derived fluid may have led to As and S (Maacha, 1994 ; Maacha et al., 1998 ; Maacha, 2013). It is also suggested that black shale of the Imiter Group could be the source of all metals and As (Bouabdellah et al., 2016). (7) The sequence of mineral precipitation with decreasing temperatures and salinities within the advancing paragenetic sequence could also have been driven by the redox-dependent solubility of Co and Ni (Scholten et al., 2018). Considering the existence of brannerite and the negative Eu anomalies in carbonates associated with Co-Ni arsenide-sulfarsenide ores, a reducing environment for mineral precipitation has been proposed (Oberthür et al., 2009). (8) The sulfur isotopic composition of sulfides (pyrite, chalcopyrite, sphalerite), precipitated after arsenides and sulfarsenides, is centred on c. 3‰ with outliers down to -32.2‰ (Maacha et al., 1998; Levresse, 2001; Dolansky, 2007). While most of the values could be compatible with the leached H_2S derived from magmatic sulfides, the outliers could be explained by H_2S being supplied and derived from the leaching of sulfides of biogenic origin, i.e. a source of sulfur prevailing in the organic-rich shales recommended as metallic sources (Bouabdellah et al., 2016).

(3) Outigua et al. (2020) did an interesting piece of research work on the Sidi M'Barek (Draa Sfar) massive sulfide deposits in central Jebilet (North of Marrakech, Morocco). It has been extensively studied using various techniques, from geophysical exploration to geochemistry and petrology (Moreno et al., 2008; Jaffal et al., 2010; Rziki et al., 2012 ; Bouabdellah et al., 2016 ; Bajdi et al., ; Essaifi et al., 2019 ; Soulaimani et al., 2020). Indeed, Cu-rich lenses, in which gold is being recovered profitably as a by-product, are the continuation of the Zn-rich lens representing the northern prolongation of the Draa Sfar volcanogenic massive sulfide deposit. The previous studies on the Draa Sfar deposit were concentrated on the Zn-rich lens (Hibti, 2001; Ben Aissi et al., 2005; Moreno et al., 2008; Rziki, 2012). At Sidi M'Barek, this Zn-rich lens, NNE-trending, is composed of massive sulfides forming a 400 m long and a thickness of ~5 m, dismembered by cross-faults into several smaller lenses. The Cu-rich massive sulfides, 150 m long and 10 m thick, form several N-S to NNE subvertical small lenses. They host massive pyrrhotite containing disseminations of chalcopyrite or banded ore with alternation of chalcopyrite and pyrite- and/or pyrrhotiterich bands. This deposit was classified as a VMS deposit (Belkabir et al., 2008; Marcoux et al., 2008; Moreno et al., 2008), but a feeder or stockwork sulfide zone has not been identified. Cu-rich mineralization is composed of numerous structurally controlled veins whose morphology suits that of a lode rather than that of a stratiform orebody. In these Cu- and Zn-rich orebodies pyrrhotite, however coarser within Cu-rich lenses, is deformed and recrystallized. The authors showed that is crosscut and replaced by pyrite infilling veins, where pyrite crystallizes also along the S_1 cleavage and in pressure shadows around bioclasts in the disseminated ore. In terms of hydrothemal fluids, lead isotopic signature indicates two types of fluids involved in the Draa Sfar deposit: a less c. 18.30 (more c. 19.01) radiogenic fluid ($^{206}Pb/^{204}Pb$) that formed the Zn-rich (Cu-rich) lens, respectively (Marcoux et al., 2008). From initial Zn-rich to subsequent more Cu-rich orebodies, hydrothermal fluids circulation may either have changed to reflect a different source rock or increased in temperature to dissolve and carry copper. In addition, the Zn-rich lens is enriched in silver, lead and arsenic, whereas in the Cu-rich lens, higher concentrations of cobalt and gold can be observed.

The Cu-rich mineralized bodies can be interpreted as being derived from syn- to post-tectonic mobilization of dispersed metals in the host rocks, probably interacting with metamorphic remobilization of pretectonic, massive and disseminated mineralization. Finally, Sidi M'Barek ore deposits can be considered as remobilized, pre-tectonic Zn-Pb systems that have been partially overprinted and further remobilized by syntectonic Cu-Au systems.

(4) The paper of **Hallarou et al. (2020a)** deals with the Liptako (Niger) locality where the Kourki Paleoproterozoic porphyry Cu-Mo deposits are revisited. A petrological analysis was performed on various facies namely (i) granitoids, (ii) gabbros, clastic sediments, schists, (iii) gneiss panels included within granitoids and (iv) an NW-SE-trending dolerite dyke crosscutting both previous facies. Based on field observations and thin sections, the authors show that epidote occurs as veins/veinlets within mineralized zones whereas molybdenite is in the form of aggregates of elongated crystals, disseminated randomly in the gangue. Molybdenite is also found in the form of nuggets in the veins of grey quartz, but sometimes disseminated in granodiorites. Most of the Cu-Mo mineralization can be found within hydrothermal breccias, filled with quartz veins and disseminated in the porphyry diorite and the quartz-diorite stockworks. The mineralogical assemblage is marked by the predominance of pyrite, molybdenite, chalcopyrite and quartz. Networks resembling stockwork veinlets rich in quartz and carbonate are also abundant. Most of them are mineralized, with chalcopyrite and a little molybdenite. Some gold values that were found have been discovered in the granodiorites of Kourki. Mo-Cu±Au metal assemblage and the mineralization style (hydrothermal, stockworks, breccias) are characteristic of an arc-type porphyry deposit.

The porphyry Cu-Mo deposits are characterized by the significant development of alteration zones that affect the entire mineralized zone. They also affect the host of porphyry intrusions. Generally, four types of alteration are found in porphyry Cu-Mo deposits: potassic, phyllitic, argillic and propylitic (Wilkin and Bornhorst, 1992). Field and microscopic observations indicate : (i) sericitization, (ii) epidotization and (iii) propylitic types of hydrothermal alterations.

A geochemical study using major and trace elements including REE is also presented on Monzodiorite quarzitic, granodiorite and microgranodiorite. The main results show that Kourki rocks constitute a calc-alkaline lineage, corresponding to granodiorites and quartzitic monzodiorites. REE analysis show for all the granitoids a strong homogeneity as in the case of the major elements, with a molybdenum grade ranging between 1.03 and 302.94 ppm with the highest content within monzodiorite. Meanwhile the Zr grade, ranging between 74.40 and 210.67 ppm, unusual in felsic rocks (here monzodiorite) may reach 207.27 ppm, corroborating the occurrence of chromite.

Finally, a genetic model was proposed for the Kourki granitoids, probably derived from partial melting of a metasomatized garnet-bearing amphibole rock with a crustal component, emplaced at ~2.137 Ga (Léger et al., 1992). Based on the isotopic analysis (Hallarou et al., 2020b), the host rock pyrites of the Cu-Mo mineralization have been dated between 2110±51 and 2158±51 Ma by the Re-Os isotopic system, consistent with the granitoids age. This occurred during the D_1 tectonic phase upstream of the Eburnean Orogeny, hence creating a juvenile Paleoproterozoic crust. Such magmatic accretionary system related to the emplacement of tholeiitic plumes in an ocean basin, formed plateaus (Soumaila et al., 2008). The oceanic crust subducted beneath the continental crust, accompanied by calc-alkaline volcanism. The island arcs induced from the intra-oceanic subduction accreted on the Archean formations. The The Kourki porphyry Cu-Mo deposit which represents the result of episodic geological events related to magma cooling, thus formed in an island arc-type subduction context.

(5) Tchaptchet et al. (2020) worked on the morphological, mineral and geochemical characterization of soil profiles to check, through trends and degrees of intensity, the role of tropical weathering as a tool for mineralizations (lithogenic concentrations of useful elements and occurrence of residual ore deposits). In fact, intensity of weathering depends strongly on climate and tectonic activity, among other factors. The Central African Fold Belt (CAFB), resulted from the convergence of three main cratonic blocs: the São Francisco-Congo Craton, the WAC and the Saharan metacraton Bloc. It was strongly affected by tectonics during the Pan-African Orogeny (600-500 Ma), leading to a complex metamorphism with various grades of metamorphic rocks, including orthogneisses, amphibolites, micaschists, mica-bearing quartzites, hornfels, quartzite veins and mylonitic zones (Soba et al., 1991; Ngako et al., 2003, 2008; Toteu et al., 2006; Ganwa et al., 2008, 2011; Njonfang et al., 2008; Kankeu et al., 2009, 2012). The northeastern part of the CAFB is characterized by an important mineralization potential (Freyssinet et al., 1989; Ntep, 1993, 1994; Ntep et al., 2001; Suh et al., 2006; Toteu et al., 2006; Fon et al., 2012; Omang et al., 2014, 2015; Vishiti et al., 2015, 2017; Ebot et al., 2016), resulting from hydrothermalism (Holler and Ghandi, 1995; Li, 2001). On this part of the mobile belt, south of the Adamaoua Plateau (central Cameroon), the authors chose seven soil profiles that developed on four types of rocks in the Meïganga area. They present some mineralization indices to trace the pathway of minerals, their chemical element mobilization and evolution to further evaluate the occurrence of residual ore deposits.

A digital elevation model (DEM), covering an area of ~12,245 km^2, shows three morphological landscapes: upper, intermediate and lower, with altitudes between 1200 and 1500 m asl, 900 and 1200 m asl, and 600 and 900 m asl, respectively.

Based on the weathering patterns at Meïganga, the mineral association reveals high contents (up to 22.3%) and the recurrence of kaolinite as the main secondary mineral. The dominant rock weathering process, i.e. strong hydrolysis, during which part of the silica, but almost all of the alkali and alkaline earth elements are leached, causing in situ crystallization of kaolinite, induces shallow weathered soil profiles (<4 m thick) (Nahon, 1991; Shoji et al., 1993; Dubroeucq et al., 1998). In order to assess the weathering trend and intensity at Meïganga, valuable weathering parameters (chemical index of alteration, CIA; weathering index of Parker, WIP ; total reserve in bases, TRB ; silica exportation ratio, Ki,), SiO_2- Al_2O_3-Fe_2O_3 ternary and laterites classification diagrams were used by the authors. They demonstrated that in the soil profiles, the TRB and WIP parameters globally decrease upward (TRB : 416 to 11 $mg.kg^{-1}$; WIP, 56 to 4%), except in the soil profile on quartzite veins (TRB : 2 to 100 mg kg−1; WIP : 0 to 29%), which may be attributed to contamination by alkali and alkaline earth elements during lateral migrations since located in lowlands (~930 m high). While the CIA (65-92%) and Ki (2-9) values in almost all profiles indicate intense rock weathering, which can result from oscillating periods of hot and humid tropical climate with >1500 mm of annual rainfall that affected the Adamaoua Plateau between Eocene and Holocene, maintaining the subsoil well-drained in permanent humid conditions favourable to intense leaching. The authors concluded that kaolinization remains the major soil-forming process in this area, regardless of the rock.

Micaschists and quartzite veins are believed to host minerals such as graphite (C), gold (Au), zinc (Zn), copper (Cu), lead (Pb), barium (Ba), tungsten (W), arsenic (As), uranium (U) and diamond (C) (Ntep, 1993; Vishiti et al., 2015, 2017; Ebot et al., 2016). The granites also contain gold (Au), sapphire (Al_2O_3), monazite [(Ce, La, Nd, Th)PO_4], silver (Ag), molybdenum (Mo), lead (Pb), tin (Sn), manganese (Mn), arsenic (As) and uranium (U) (Ntep, 1993, 1994). The exploitable U concentrations (1500-2000 ppm) in the soil profiles on quartzite veins and micaschists are above the exploitable limit (1000 ppm) and thus can be compared to the residual ore deposits of U at Meïganga (Omang et al., 2014, 2015). Major elements that can be considered as indicators of mineralization are: Fe_2O_3 for Mo; Al_2O_3 for Nb, Mo, W, Nb and U; and TiO_2 for Nb, V and Cr.

(6) Gold is found mostly in greenstone belts, especially in the interfaces of the Birimian volcanic and volcanoclastics (Burkina Faso, Côte d'Ivoire, Ghana, Mali, Senegal, etc.)(e.g., Davis et al., 1994; Béziat, et al., 2008; Ballo et al., 2016; Dabo et al., 2016; Augustin and Gaboury, 2017;), but also in the contacts between both these formations, affected by shear zones (Milési et al., 1989; Houssou, 2013; Ouattara, 2015; Ouattara et al., 2015; Houssou et al., 2017; Ouattara et al., 2018a). The paper of **Ouattara et al. (2020)** concerns gold mineralization in the Oumé-Fettèkro greenstone belt, one of the largest Precambrian belts (300 km long and 40-5 km wide) of Côte d'Ivoire. This greenstone belt, composed of NNE-SSW schist and quartzite, sandstone and conglomerates, is affected by different injections of meta-basites and acidites (Yacé, 1982; Lemoine, 1988; Mortimer, 1990; Daouda, 1998; Houssou, 2013, Ouattara, 2015; Ouattara et al., 2015; Houssou et al., 2017).

The authors concentrated on the Bonikro deposit to try establish a relationship with the shear zones. This is a particular area where sheared granodiorite hosts gold within areas of faulting and "boudinaged". The Fettèkro is one of the numerous greenstone belts NE to ENE trending along with their shear zones, considered as the most productive gold belt in Côte d'Ivoire. In its southern part, namely the Oumé-Fettèkro greenstone belt, extensive exploration resulted in the discovery of four gold deposits: Bonikro (15.9 kt at 1.8 g/t) (Ouattara, 2015; Ouattara et al., 2018a, b), Agbahou (Houssou, 2013; Houssou et al., 2017), Dougbafla-Bandama (Ouattara et al., 2017) and Hiré (Gnanzou, 2006). The first Bonikro pit, located in the southern part of the deposit where the shear zone can be seen (Ouattara et al., 2018a), the higher-grade ores were found around NNE quartz veins. In the second and main pit, the shear zone appears in the central part. The authors try to understand the influence of the Bonikro shear zone (BSZ) on the mineralization, hence on gold deposits, combining both fieldwork and laboratory analysis, focused on mineralized veins.

Bonikro open-pit benches were used to investigate (micro)structural observations and core analyses (polarizing microscope¸ scanning electron microscope) for comparison. Fluorescent minerals between scheelite-bearing and nonscheelite- bearing within the veins were separated through a mineralight lamp UVG-47.

The distribution of gold in the Bonikro deposit occurs along the BSZ, its related structures and sheared rocks (e.g. faults, veins and schistosities). Gold is hosted exclusively in the N-S-trending BSZ corridor, dominated by quartz and pyrite, where contact is established between both primary lithologies, i.e., the eastern volcanics and the western volcaniclastics and sediments. S_2 (pluton-basalt contact) is a key indicator of mineralization, recognizable by its abundant pyrite, and indicating that the gold enrichment is post-magmatic and syn- to post-tectonic. In fact, the intensity of shearing in the basalt controls ore grade increase, since calcite is replaced successively by dolomite and ankerite in the areas where pyrite and pyrrhotite are abundant. Hence, higher-grade ore is found in intensely sheared zones. Sheeted, planar and transversal veins appear to control most of the gold deposits. The sheeted veins, N000° to N045° oriented, are the oldest at Bonikro. They cut potassic feldspar megacrystals, showing that they were definitely formed after the magmatic events. These veins are the main hosts for scheelite and most of the visible gold. The planar veins, N009° to N018° oriented, are of secondary type, comprising quartz associated with powellite and fractured pyrite. Finally, transversal veins, N120° to N150° oriented, are the youngest vein type. They consist of larger quartz veins cutting the two previously mineralized types of veins and are composed of milky quartz, calcite, albite, biotite and sulfides (molybdenite up to 5%). The molybdenite is sheared and unevenly distributed around broken pyrites in the zones where the transversal veins cut the planar or sheeted veins.

In northern Bonikro, mineralization is correlated with the three domains of the BSZ : (i) the first controls the contact between sediments and granodiorite, N-W oriented , (ii) the second, N-S oriented, within the granodiorite, and (iii) the third, N-E trending, represents the interface between pluton and basalt. These changes in orientation of the granodiorite and the contacts between intrusives and primary lithologies have influenced the fluid circulation pathways and thus gold deposits. Strain slips are also present in the northern part of the pit; they formed from the stress that resulted from the intrusive setting and the effects of fractures.

The structural history of the Bonikro gold deposit can be summarized as follows: (i) regional folding event that set up the N-E-trending structures; (ii) regional shear zone, i.e., Bonikro Shear Zone (BSZ), redirected the primary faults, and (iii) occurrence of secondary structures with dextral thrust veins that reactivated shear faults and fractures, and controlled mineralizing fluid flows.

Section 2: Geodynamics and emplacement mechanisms

7) The research work of **Aïfa and Merabet (2020)** was undertaken in the Yetti–Eglab terranes on N-S oriented Proterozoic intrusions to try (i) to compute new palaeopoles and build an apparent polar wander Path (APWP) for the West African Craton (WAC) and (ii) to better constrain the WAC's geodynamic evolution. In fact, a paleolatitude vs. age diagram in the light of other rare paleopoles available in closeby terranes, blocks or (micro)plates, together with previous geological and radiochronological studies, suggest that this craton could have participated successively in the assembly of the Columbia and Rodinia supercontinents (Aïfa et al., 2001; Lefort and Aïfa, 2001, 2002; Lefort et al., 2004; Kouyaté et al., 2013).

The Reguibat uplift is an area of 1500x400 km^2, covered, in its northern and southern parts, by the Paleozoic Tindouf and Taoudeni basins. It is composed of the Yetti and the Eglab zones, almost undisturbed since 2.1 Ga, and not affected by the Pan-African orogeny (600 Ma) that borders it. In the Eglab area eastward, subtle extensional tectonics can be recognized, highlighted by a transgressive stromatolite-bearing sedimentary cover : the Hank Formation (c. 875–890 Ma, Clauer and Bonhomme, 1971; Bertrand-Sarfati, 1972; Bertrand-Sarfati and Moussine-Pouchkine, 1992 ; Aïfa et al., 1993 ; Tewari and Seckbach, 2011). This formation deposited before the opening of the Pharusian Ocean (Caby and Andreopoulos-Renaud, 1989; Helmstaedt and Scott, 1992 : Condie, 1992, 2003; Condie et al., 2000) at ~800 Ma. Some E-W-tilted blocks supported by listric normal faults can be observed in the field, separated by large N-S-oriented doleritic dyke swarms and represent the westernmost remnants of the Pharusian continental margin and foreland. In the easternmost part of this zone, some of the dykes intruding the Early Proterozoic and the Archean basement were probably emplaced during an extensional event predating the opening of the Pharusian Ocean (Condie, 1992; Lefort et al., 1994; dos Santos et al., 2008). Several magmatic episodes are evidenced (Sabaté and Lameyre, 1973; Kahoui et al., 1996; Drareni et al., 1995; Kahoui and Mahdjoub, 2004; Peucat et al., 2005; Merabet et al., 2014, 2016, 2020).

The dyke package, which was feeding the post-tectonic Eglab volcanics, gives a preliminary age of 1948±9 Ma on baddeleyite using the $^{207}Pb/^{206}Pb$ dating. This result broadly fits with the previous Rb/Sr dating of the post-tectonic volcanics at 1.99±0.03 Ga (Sabaté, 1978, 1979). Dating carried out on zircons of host rocks (quartz–dioritic gneisses) were also made and fits with previous results (Mahdjoub et al., 1994; ages in the range of 2.21–2.18 Ga; Peucat et al., 2005). Taking account of dating limitations at older ages, an error of c. 5-10 Ma will not bring major distortions in the APWP path. A rough comparison of the current palaeomagnetic data with those previously determined (e.g. Sabaté and Lomax, 1975; Aïfa et al., 1993) is necessary. Because no contact test was generally available for thes sampled dykes, a detailed rock magnetic study was performed for the identification and stability of the magnetic carriers. The main magnetic mineral is multidomain stable magnetite and/or titanomagnetite, however hematite, pyrrhotite and goetite may also occur.

In terms of paleomagnetic directions, several paleopoles were computed, considering palaeolatitudes v. ages, to build suitable interpretations in terms of geodynamics:

(i) The Yetti-Eglab zones, the deeper basement of which is made from Archean Chegga gneisses (Drareni et al., 1995), were probably separated by an ocean because they follow different paths between 2.1 and 2.08 Ga. However, a c. 2.73 Ga oceanic relic, composed of garnet– hornblende banded grey gneisses, is interpreted as Archean oceanic crust in the Eglab massif (Peucat et al., 2005). It could be associated with rifting, crustal breakup and oceanization of the 3.0-3.6 Ga old craton during the Liberian events (Peucat et al., 2005; Taylor et al., 2019).

(ii) A possible existence of oceanic crust supported by a calcalkaline volcanic arc at ~2.03 Ga (Sabaté, 1978). Given the the K_2O/SiO_2 geochemical gradient, subduction of this crust was dipping eastwards (Lefort and Aïfa, 2002; Peucat et al., 2005). Some magnetizations possibly predate the collision between the two terranes that generated the Aftout granites (1.92 Ga) (Peucat et al., 2005), slightly predates the amalgamation of cratons to form the Columbia Supercontinent (Rogers and Santosh, 2002a, b, 2003, 2004). Such crustal thickening could be indicative of a diamondiferous area (Kahoui et al., 2008, 2012). This accretion may have developed whilst the WAC was drifting close to the northern low latitudes. A very large volume of granites (the Aftout granites) witness the existence of an oceanic closure at this time. The main crustal break (the Yetti-Eglab "suture zone") known in the field between these two domains (Sabaté, 1978) probably represents a microplate boundary.

(iii) The palaeopoles, dated around 1.8 Ga (Rio de la Plata Craton [RPC], Halls et al., 2001) suggest, because there is no Precambrian orogeny between the WAC and the Rio de la Plata Craton, no collision, although they were located at approximately the same palaeolatitude. They correspond either to the collapse of the Birimian and contemporaneous orogens or to the very beginning of the fragmentation of Columbia.

(iv) The palaeopole dated at 1.5 Ga (Sabaté and Lomax , 1975) obtained on the younger dyke generation may correspond with a period of extension, probably contemporaneous with the collapse of the Birimian orogen. It may correspond to the beginning or the continuation of the fragmentation of Columbia.

(v) The palaeopole obtained from the transgressive Hank Formation shows that the WAC was, at c. 900 Ma, located at low and warm latitudes (31°) since the stromatolites were able to develop on a continental margin. Compared with the data compiled by Onstott and Dorbor (1987), nearly the same path for the WAC from 2.2 to 1.9 Ga is established.

The similarities in the pole position for Baltica and for the WAC at 0.95-0.89 Ga (Aïfa et al., 1993), 1.5 Ga (Pesonen et al., 1991) and 1.79 Ga suggest that the WAC and Baltica have been drifting at similar latitudes for a very long period of time. However, they have probably never been attached to one another before their amalgamation to the Rodinia Supercontinent at c. 1 Ga, since the Grenvillian orogen that affected Baltica is absent in western Africa. The lack of deformation in the c. 1 Ga Hank cover of the Reguibat uplift suggests that the WAC never collided completely with Rodinia (Lefort et al., 2004).

(8) The manuscript of **Kwékam et al. (2020)** deals with I-type granites of Dschang (S-W Cameroon). Using Laser ablation U-Th-Pb geochronology, whole rock geochemical, Rb-Sr and Sm-Nd isotopic analyses, these biotite (BG) and magnetite (MG) granites were dated at ~578 +7/-11 Ma and ~563 +8/-3 Ma, respectively. They are high-K calc-alkaline and weakly hyperaluminous with ferroan affinity (Kwékam et al., 2015). According to similar magnetite granites within both Dschang and Nkambe regions, they could belong to a single Paleoproterozoic domain, rich in iron mineralization. In fact, BG and MG Nd isotopes display ε_{Nd} from -16 to -18 and from -15 to -17 with Nd T_{DM} indicating Paleoproterozoic ages in the ranges 2112-1923 Ma and 1875-1713 Ma, respectively. They are of a potential metallogeny source of Cu, Pb, Zn and Mo metals, typically post-collisional, with a subduction signature probably being inherited from their protoliths. The authors also show that the inherited zircon U-Pb age of these granites are at the origin of remobilization of an old Paleoproterozoic crust similar to the BIF of the Nyong series of the Congo Craton. The geochemical results indicate a crustal growth during the late Pan-African Orogeny. Dschang granites are typically derived from partial melting of older rock in the crust (Roberts and Clemens, 1993; Barbarin, 1999; Frost et al., 2001). In terms of petrogenesis, the Dschang MG granites are characteristics of upper crustal granites (Kemp and Hawkesworth, 2003).

The age of Dschang granites (578 +6/-11 and 563 +8/-3 Ma) is consistent with their emplacement after the end of arc-related magmatism and subsequent collision between the Congo-São Franciscco Craton and the Sahara Metacraton during the lateral wrench movements along the N70°E Central Cameroon sinistral shear zone (CCSZ) (Ngako et al., 2008). Such emplacement age coincides with the metamorphism and D_4 deformation event along the CCSZ (Bouyo Houketchang et al., 2009; Tchaptchet Tchato et al., 2009; Kwékam et al., 2013; Tcheumenak Kouémo et al., 2014). These results revealed, through injection of mantle melts within the upper continental crust, a remobilization of the older crust, here Paleoproterozoic in age. It would have triggered the dispersion of ante-Panafrican mineralizations.

(9) Amadou et al. (2020) studied the Proterozoic deposits of the Firgoun region within the Gourma and Taoudeni basins (west Niger) through field observations, i.e. sedimentological and structural data analysis. The Gourma Basin, considered as a sedimentary prism with terrigenous and carbonate infills, is marked by a high subsidence rate with a thick sedimentary pile (>8000 m) on top of a major unconformity on Paleoproterozoic terrains, southeastern edge of the WAC. The Gourma Basin recorded two stages of evolution with an increase in the Pan-African deformation rate eastwards: (i) an aulacogenous stage (Moussine-Pouchkine and Bertrand-Sarfati, 1978) or linked to the opening of the Neoproterozoic Ocean [870-800 Ma] (Black et al., 1979) ; (ii) a compressive tectonic event, associated with the development of thrust nappes [folds and tangential structures] (Caby, 1989).

The Firgoun area deposits were dated from Meso- to Neo-proterozoic (Miningou et al., 2010, 2017; Konaté et al., 2018). They include two lithostratigraphic units: (i) the basal 'Firgoun Sandstone Formation', unconformably overlying the Birimian basement and (ii) the uppermost 'Béli-Garous Formation' corresponding to a sedimentary sequence comprising glacial and non-glacial lithofacies. The authors described accurately these outcrops in the field and through microscopic analysis. They show that 'Firgoun Sandstone Formation' presents symmetric ripples associated with oblique bedding, asymmetric current ripples, flat-crested sinuous or undulatory ripples, herring bone structures and HCS, suggesting a *shallow marine environment with fluvial episodes*. While 'Béli-Garous Formation' consists of (a) several sedimentary structures (symmetric ripples, herring bone structures and hummocky cross-stratification) characteristic of *shallow marine context*, (b) diamictite interbeds-carbonates-silexites and other glacial features (stepped fractures and cryoturbations) suggesting *glacial to marine environment*. According to their characteristics, the lowermost sedimentation of 'Firgoun Sandstone Formation' consists of *fluvial to marine environments that evolved vertically from marine to glacial environments*.

The Firgoun area deposits also show brittle and ductile deformations in the field, mainly fractures, and folds and schistosity, respectively. The brittle deformation has affected all the basal deposits inducing normal faulting acting during sedimentation (sandstones displaying secondary fractures, oriented 40-60°N, with quartz infills) and post-depositional thrusts, oriented 60-80°N, associated with westerly verging nappes. The ductile deformation exhibits isopachous folds (concentric folds, with axial planes, oriented 30-50°N and dipping 40-50°NE), sometimes accompanied by microfractures of variable direction (55°N, 140-150°N). The 'Béli-Garous Formation', overlying the'Sandstone of Firgoun Formation', records brittle deformation, characterized by intragranular fractures (infilled with manganese or ferromanganese oxides) in cataclastically deformed porous sandstone. However, in lithofacies Fr6, two categories of deformation structures have been observed. These are anisopachous folds for which the axial plane mean orientations are 30-50°N 45-40°NE with plunging axes 10-20°NE. On a regional scale, they form a network of elongated parallel hills, orientaed 45°N.

In terms of deformation phases, three phases were recorded : (i) an extensional deformation stage D_1, marked in the basal deposits by brittle deformation structures exhibiting syn-sedimentary normal faults, with a stretching direction trending 140°N, possibly linked to the Neoproterozoic Ocean opening northeastwards. (ii) A first NW-SE compressive episode D_{2a}, marked by isopachous folds in the basal deposits, has affected most of the Firgoun area deposits. According to their constant layer thickness, the isopachous folds are post-depositional deformation structures. In the uppermost deposits, the folding related to D_{2a} episode was marked by anisopachous open folds, exhibiting layer thickness variations, thus syn-depositional. (iii) A second NE-SW compressive episode D_{2b}, also marked by brittle structures, such as thrusts and reverse faults, crosscutting all the previous structures. The intragranular fractures in cataclastically deformed porous sandstones are linked to the compressive deformation episode D_{2b}.

The single U-Pb geochronological age recorded in the Firgoun lowermost sediments is ~1800 Ma (Konaté et al., 2018). The uppermost siliciclastic sediments of the Firgoun region could be Late Cryogenian (630-610 Ma), since they exhibit some lithological similarities to the Late Cryogenian sediments of the Taoudeni, Gourma and Volta Basins. Finally, the authors agree that the compressive deformation phases recorded in the Firgoun area are Pan-African in age. Such tectonic events, particularly those of the Pan-African orogeny, may have had a direct influence on the distribution and uprising of the continental blocks and consequently on the origin of the major Neoproterozoic climatic changes. For the Gourma aulacogen, a possible relationship between Neoproterozoic sedimentation and the breakup of the Rodinia Supercontinent has also been proposed (Michard et al., 2008).

The Neoproterozoic to Cambrian deposits within the Taoudeni Basin and its surroundings, including glacial deposits of West Africa, could be partly controlled by the Pan-African events, consistent with the sedimentary record of the Pan-African events in the Firgoun region.

(10) The paper of **Baraou and Konaté (2020)** deals with new radiometric dating from south Maradi formations, southern Niger. They formed during the Pan-African Orogeny (between 750 and 450 Ma, Ajibade and Wright, 1989) as a result of the convergence-collision of the WAC, the Congo Craton, the Saharan Metacraton and the São Francisco Craton to amalgamate in West Gondwana (Black and Liégeois, 1993; Abdelsalam et al., 2002; Caby, 2003; Liégeois et al., 2003; PRDSM, 2005). However, the age spread of the Pan-African Orogeny during the convergence of East and West Gondwana is a matter of debate. Some authors have suggested ages ranging from 750 to 450 Ma (Ogezi, 1977 ; Van Breemen et al., 1977 ; Ajibade and Wright, 1989), while others have argued that the Trans-Saharan belt was formed between 750 and 500 Ma (Caby, 1989 ; Castaing et al., 1993 ; Stern, 1994, Villeneuve and Cornée, 1994 ; Trompette, 1997 ; Abdelsalam et al., 2002), whereas Mc Curry (1976), based on K-Ar dating of mica in metasediments and volcanics, proposed ages varying from 600 to 450 Ma. The southern Maradi Province forms an alternatively juxtaposed domain (synclinal form) of four bands with a NE-SW-trend of schist belts: (i) the Maraka Schist Belt (MSB), (ii) the Eastern Goumata Schist Belt (GSB), (iii) the Garin Liman Schist Belt (GLSB), and (iv) the Maidaparo Schist Belt (MpSB). They are composed of gneiss, mylonitic granitic gneiss, quartzites and post-tectonic granites including pegmatites dykes (Mignon, 1970; PRDSM, 2005; Baraou et al., 2018).

As no zircon was found in the collected samples of mylonitic gneiss and porphyroid granites, the K-Ar method was used. SEM images of schist and cathodoluminescence (CL) images of porphyritic gneiss exhibit zircon grains for laser ablation inductively coupled plasma mass spectrometry (LA-ICP-MS). They were used to determine the age of magmatism and/or metamorphism of different petrographical facies, through K-Ar and U-Pb methods on zircon.

Dan Issa migmatite gneiss is characterized by a wide variety of petrographical facies, including palaeosomes of porphyritic gneiss and granitic leucosome. Microscopic analysis of the palaeosomal component shows mineral assemblages comprising quartz, orthoclase, microcline, sodium plagioclase and biotite. The CL image from the palaeosome of migmatite gneiss shows zircon grains. The core of some zircons has strong luminescence (inherited nuclei) and some have low luminescence (altered nuclei). The Th/U ratio varies from low (0.191-0.394) to high (0.493-0.808) values, revealing crystallized (inherited) and recrystallized (altered) zircons, respectively. According to Williams and Claesson (1987), the Th/U ratios of metamorphic (magmatic) zircons are often low (high). The concordia diagram for all zircons analysed indicates two weighted averages for the mean U-Pb ages: (i) one with an average of 638.3±3.0 Ma (MSWD=5.4, high average) which could represent zircon crystallization (igneous crystallization) and (ii) the other with an average of 589.6±1.9 Ma (MSWD=0.39, low average), could correspond to the age of the zircon overgrowth (remobilized system) during a Pan-African high-grade metamorphism.

Similar Ar-Ar ages of 565±5 Ma on hornblende, and U-Pb ages of 589±11 and 605±10 Ma on zircon were obtained on this type of gneiss in the Nigerian Pan-African Province (Dada et al., 1993 ; Ferré et al., 2002), and in northern Benin (Adissin Glodji, 2012).

Zircons dating from the schist belt rocks of Maraka by U-Pb method gave an age of 617.9±2.8 Ma (MSWD = 2.3). U-Pb zircons can be interpreted as a detrital age for the volcanic material in the sediments. In addition, this volcanic material was interpreted as the schist protolith, and is from arc-type volcanism. Radiometric dating of feldspars of the Rourouka porphyroid granite by the K-Ar method, on whole rock, gave an age of 508±10 Ma, which is similar to the metamorphic age of the Maraka schist (505±15 Ma) using the K-Ar method on whole rock. As this porphyritic granite is undeformed, the obtained age could correspond to cooling of the granite intrusion during the Early Paleozoic (Cambrian).

Garin Wali and Fiawa mylonitic gneisses are affected by N-S to N20° mylonitic foliation with a sinistral S-C fabric. Radiometric dating of feldspars from these gneisses gave K-Ar ages of 491±10 Ma and 475±10 Ma, respectively. They correspond to an Early Paleozoic (Ordovician) reactivation and are compatible with previous ages on the porphyroid granite of Rourouka ((510±20 Ma).

Finally, the south Maradi Pan-African formation ages range from 638.3±3.0 Ma (Neoproterozoic) to 475±10 Ma (Ordovician), revealing the polycyclic character of the Pan-African events. The U-Pb method yielded older ages from migmatite gneiss (638.3±3.0 Ma) and schist (617.9±2.8 Ma), while the younger ages are obtained by the K-Ar method from mylonitic gneiss (491±10 and 475±10 Ma) and granite (508±10 Ma). In migmatite gneiss, the U-Pb ages (638.3±3.0 and 589.6±1.9 Ma) obtained on zircons do not allow attributing a Paleoproterozoic age to their protolith. Such a lack of Paleoproterozoic rocks could be linked to significant remobilization during the Neoproterozoic and Early Paleozoic in the West Gondwana amalgamation.

(11) In the paper of **Gouedji et al. (2020),** the mafic-ultramafic Samapleu intrusion, west of Côte d'Ivoire, is investigated to characterize its petrology, geochemistry and metamorphism. Base metal deposits (Ni, Cu and Co), platinum group elements (PGE) and chromite are associated with this intrusion. In fact, it is a feeder dyke of the Yacouba layered complex composed of three assemblages (Gouedji et al., 2014 ; Ouattara, 1998). The Yacouba layered complex forms dismembered and stretched assemblages that extend for more than 25 km in a corridor from Yepleu-Bounta to Samapleu-Yorodougou village. It consists of layered assemblages composed of mafic-ultramafic sequences with petrographic markers of high/ultrahigh-temperature metamorphism and coeval deformation (Gouedji et al. 2014, 2018), and locally magnetite-rich anorthosite units. Its geodynamic context (2.09 Ga) will be better understood in the frame of its geochemical and metamorphic characteristics, and the relationship with the granulite gneiss host (P-T conditions) during emplacement and recrystallization within the Man Archean domain at 2.8 Ga. A more than 40 m thick layer of laterite alteration covers the Samapleu intrusion, so drilling crosscuts the ultramafic, mafic and the hybrid (remains of the granulite host) (Gouedji et al., 2014, 2018) units. Combined with the mineralogy and geochemistry, the P-T-t path of metamorphism through pseudosections of diagnostic assemblages of these units has been investigated.

The authors describe in detail (i) the ultramafic, mafic and hybrid units which are composed of (a) peridotite, chromitite, spinel websterite, olivine and plagioclase, (b) gabbro-norite, norite and anorthosite, and (c) grey lithofacies with a mineralogical composition varying from noritic to anorthositic pole, respectively. The samples from the hybrid lithofacies, with very low TiO_2, Na_2O, MnO and K_2O contents, were used to quantify the P-T conditions of the Samapleu intrusion emplacement. Their wide variability in the geochemistry of major oxides reflects the possible mingling of mafic-ultramafic intrusion and host rock. The phase relation modelling suggests that the hybrid lithofacies at the contact of the Samapleu intrusion preserves evidence of ultrahigh-temperature (≥1000°C) and pressure (~9 kbar) conditions. It is followed by near isobaric cooling down to 750-800°C at 7-8 kbar, suggesting that these metamorphic conditions and the development of the hydrid lithofacies are coeval with the Samapleu intrusion emplacement. In addition, the high MgO (10-13%) levels recorded indicate that Samapleu magmas were relatively hot (Precambrian thermal gradient of ~50°C/km; Chardon, 1997), implying an emplacement depth of the intrusion of 22 km (lower crust) with a crystallization temperature of 1100-1200°C. An Eburnean age (2.09 Ga, U-Pb age obtained on rutile) was obtained on hybrid lithofacies, which would be the age of metamorphism that produced these formations (Gouedji et al., 2014).
Chondrite-normalized REE patterns of the Samapleu rocks are generally flat (REE concentrations between 1 and 10 times chondrite values), slightly enriched in LREE and relatively constant in HREE. Finally, the signatures of trace elements and REE show that they are affected by crustal contamination with a small assimilation proportion of the granulitic continental crust during its emplacement. The magma could have been emplaced by underplating and feeding from a mantle plume at the base of the continental crust.
(12) The paper of **Ilboudo et al. (2020)** aims to contribute to the understanding of the Banfora volcanic and associated intrusive rocks, loacted in the eastern margin of the Banfora Belt (BB), S-W Burkina Faso, west of the Birimian Houndé and Boromo Belts within the Léo-Man shield (WAC). Its size is 160 km long and 35 km wide, trending NNE-SSW, continues in Côte d'Ivoire, where it is called the Katiola-Marabadiassa greenstone belt and Bandama volcanosedimentary belt (Ouattara, 1998).
The geological environment is dominated by sedimentary and volcanosedimentary rocks that have undergone greenschist facies metamorphism (Baratoux et al., 2011; Metelka et al., 2011; Ilboudo et al., 2017). Several magmatic episodes with mafic, intermediate and felsic volcanic rocks cropping out on the eastern side of the belt, along a N-S trend, could make the BB a target for mineral exploration. They are intruded by gabbro, diorite and granite bodies. The Banfora, Houndé and Boromo belts exhibit similar volcanic units, in particular the eastern margin of the BB and the western margin of the Houndé Belt (Baratoux et al., 2011 ; Metelka et al., 2011). As there are few geochemical studies, the authors targeted magmatic rocks from both mafic and felsic composition. They therefore focused on: (i) the geochemical nature of the magmatic environment (self-consistency of data, magmatic series, geotectonic settings) supported by petrographic descriptions of the different facies; (ii) a geodynamic model, based on the correlation with the other belts; and (iii) assessment of the BB's potential in terms of mineral resources.
Studies based on radiometric and electromagnetic data supported the hypothesis that volcanic rocks (basalt, andesite, rhyolite)(<10%) estimated to be 2-4 km thick are intercalated with volcanosediments in the eastern part while the remaining part is composed only of volcanosediments (~90%) (Baratoux et al., 2011; Metelka et al., 2011). They are cross-cut by a syn-kinematic elongated granite emplaced throughout a major shear fault called 'the Greenville Fault' in the central part. The eastern and western sides are separated by syn-kinematic two-mica granite and granodiorite bodies along a NNE-SSW trend, coinciding with the Greenville-Ferkéssédougou-Bobo Dioulasso Shear Zone (GFBSZ), a

first-order crustal scale shear zone (Lemoine et al., 1990; Baratoux et al., 2011). The GFBSZ extends from Liberia southwards, passing through Côte d'Ivoire, and to the BB (Burkina Faso) northwards.

The granitoids intruding the belt in the Katiola-Marabadiassa area, gave radiometric ages ranging between 2123±3 and 2097±3 Ma (zircon Pb-Pb; Doumbia et al., 1998). Detrital zircons from the sedimentary rocks of the Bandama Basin were dated (Pb-Pb) at c. 2133 and 2107±7 Ma. Based on the zircon Pb-Pb ages of pre- and post-basin granitoid intrusions, their emplacement age was estimated at between 2108±12 and 2097±3 Ma. In addition to these syn-kinematic granites, the BB is cross-cut by granodioritic, dioritic (+quartz-bearing) and tonalite plutons that are responsible for local contact metamorphism.

The authors also performed rock classifications using thin sections on the sampled outcropping rocks (granitoids, mafic and felsic volcanics and associated intrusives). They were subjected to inductive coupled plasma-atomic emission spectrometry. It was found that they are mainly composed of basalt and andesite with associated mafic and felsic intrusives, altered or under greenschist or amphibolite facies metamorphism, suggesting an igneous protolith (I-type). The two-mica granite, accommodated by the GFBSZ, is sourced from sedimentary protolith (S-type). Bulk chemical (major, traces and REE, REEs) composition of the volcanic and intrusive rocks confirmed the petrologic results. These mafic volcanic and plutonic rocks are calc-alkaline, tholeiitic or komatiitic.

They interpreted the main results as follows : The nearby Houndé Belt, that shows a genetic link with the Banfora, is an ancient oceanic floor at least 8 km thick made up of tholeiitic basalts (Baratoux et al., 2011 ; Augustin and Gaboury, 2017). This floor formed above a deep mantle plume that pre-enriched basalts in gold (Weber et al., 2012). Its evolution led to the formation of an island arc during the compressive D_1 deformation phase, with a hypothetical subduction zone eastwards. During D_1, calc-alkaline magmatism developed (andesite) with TTG emplacement and sedimentary basins were formed in possible syn-deformational settings during the late Eburnean, e.g. the Tarkwaian (Ghana). Gold mineralization appeared later during transpressional phases (~2150 Ma). The BB, like the Boromo, probably has a similar geological history to the Houndé Belt and a genetic model similar for the overall belt in western Burkina Faso is supported. However, this interpretation is not supported by geochemical data as far as the BB is concerned. Rocks, ranging from tholeiitic (high-Mg+Fe) basalts, with komatiitic affinities (pyroxenolite) to dacite-rhyolite, are exposed eastwards, with an evolution from MORB to arc-type. Economically, both I- and S-type could be productive for mineral resources. Although a limited number of selected basalts at Banfora did not allow an overall assessment of their potential compared with the mineralized basalts of Mana world-class gold deposit (Houndé Belt), the geological setting shows slight similarities with the Houndé Belt although dacite and rhyolite could constitute volcanic centres at Banfora. Finally, based on the old and recent data available, the authors suggest an eight-part revision of the lithostratigraphy chronology (e.g., Ilboudo et al., 2019). Rhyolites host disseminated sulfides and are a target for gold and base metals. Generally, border granites are of metallogenic interest because they constitute a better receptacle for gold-bearing hydrothermal fluid. The authors suggest that the main targets, located on the borders of the BB, may contain orogenic gold; massive sulfide and porphyry-type deposits as well as VMS (exhalite on top of mafic-felsic volcanic activity) are documented in the Birimian system of Burkina Faso (Franklin, 1996; Gaboury and Pearson, 2008; Hein, 2016). Further, the BB should not be excluded from exploration companies (Ilboudo et al., 2017) for alluvial diamond (Castaing et al., 2003).

Section 3 : Geological, Geochemical and Geophysical modelling

(13) In the paper of **Aïfa and Lo (2020),** investigations of Precambrian subsurface structures were addressed through aeromagnetic data on the gold-bearing Tasiast area (N-W Mauritania). In fact, the inferred structures, composed of dykes and shears, are oriented mainly NNE-SSW, NW-SE and ~N120° at subsurface (Ba et al., 2020). The gold deposits are hosted along a N-S oriented dextral shear zone with an area of 70 × 15 km^2. Mineralization follows a series of reactivated thrust faults at the northern end of the Chami Greenstone Belt, including Tasiast and Piment fracture zones. They host a large proportion of the gold-bearing deposit, and are composed of banded iron formations (BIF), felsic volcanic rocks and associated clastic and mafic rocks. Tasiast-Tijirit Terrane comprises three lithostratigraphic units: (a) TTG-type granitic gneiss rocks assembled into the 'Ctel Ogmâne Complex', (b) greenstone belt lithologies assembled into the 'Lebzenia Group' and (c) late granitoid intrusions belonging to the 'Tasiast Suite'. The Tasiast ore bodies are presented as layered quartz-carbonate-albite-pyrrhotite-pyrite veins, carbonate quartz veinlets containing gold, and adjacent gold disseminated and hosted within (i) higher greenschist to amphibolite facies rocks, (ii) ribbons or BIF with magnetite-quartzite, and (iii) adjacent volcano-clastic rocks. All of these mineralization events follow a series of reactivations of reverse faults, including the fracture zones of Tasiast and Piment. The clay alteration and the high salinity of fluid inclusions suggest possible orogenetic gold deposits dated within the range 1.85-1.5 Ga (Higashihara et al., 2004; Marutani et al., 2005).

The geophysical processing of aeromagnetic data (3D Euler deconvolution, spectral analysis, etc.) using several filters provided a clear 3D subsurface image at depths up to 5 km. A structural map was derived from this investigation and corroborates the outcropping structures, either for the in situ magnetic susceptibilities or for the induced magnetic data. On the Reduced to Pole (RTP) magnetic map one can notice magnetic anomalies presenting extreme values concentrated much more on small surfaces around structures, e.g. Tasiat area, hardly visible on the Total Magnetic Intensity (TMI) map. The computed upward continuation from 500 to 2000 m with an interval of 500 m on the RTP map reveals the progressive evolution of the various structures (amplitude attenuation till disappearance of some of the anomalies) and their location at large depths. The strong magnetic susceptibilities measured in situ on BIF (25.7-35 × 10^{-3} SI) correspond to NE-SW linear structures, mainly west of Akjoujt. In addition, some NNW-SSE to N-S structures also exhibit high apparent magnetic bulk susceptibility values. To characterize the azimuthal intensity, directional derivative maps were computed with respect to X and Y, deciphering the weak (strong) azimuth structures, respectively.

Analytic signal (AS) and first derivative maps show similarities highlighted mainly within the main trending directions. But the AS map is more significant when dealing with same geometry bodies, e.g. four main linear and massive bodies can be distinguished. In addition, upward continuation and 3D-EDS maps for different elevations show that NNE–SSW linear structures disappear at 2000 m and 1000 m, respectively : either the signal-to-noise ratio is weak or no magnetic anomalies are detectable at 2000 m high.

The results of the power spectral analysis (Okubo et al., 1985 ; Tanaka et al., 1999) indicate depths>4 km (deep sources) to the S-W, and north and N-E. They follow the same behaviour, i.e. depths<120 m (shallow sources), within the same areas, while 3D-EDS maps show that the major sources (>0.5 km) are mainly in the south and the west. Such differences can be explained by materials with various magnetic susceptibility values at depth, corroborating field observations where the basement crops out to the northeast and is deeper westwards and southwards (coastal basin). Hence, the magnetic sources are much deeper southwestwards and from 3000 to 5000 m very few magnetic sources can be distinguished.

In conclusion, the authors state that the maps of the various magnetic gradients computed correspond to lengthening of dykes/abnormal contacts. The BIF west of Akjoujt may present metallotects for gold-bearing exploration and base metals deposited in paragenetic balance. A structural map is proposed showing the main linear trending structures that would correspond to Mesoarchaean and Palaeoproterozoic dykes, shears or faulting systems roughly oriented 120° N, and N-S to NNE-SSW, respectively. However, deeper basement areas can be highlighted S-W and N-E of the study area, whereas the basement topography is shallower in its centre and northwestwards. In addition, the massive bodies on the map could be granitoids, some of which crop out at different locations (Gunn et al., 1997).

(14) Nyame et al. (2020) present a paper related to Birimian Mn mineralization within the Kibi-Winneba metavolcanic belt, in the Mankwadzi area, west of Accra. Birimian terrains throughout are dominantly stratiform within host metavolcanic-metasedimentary sequences such as greenstone, phyllite and schist (quartz schist, quartz-sericite schist, etc.). This feature (or at least relicts thereof) seems to be prevalently displayed irrespective of the postformation modification that may have affected the rocks. In general, the stratiform or stratabound nature means that they are mostly conformable with the enclosing rocks (Hein and Tshibubudze, 2016), except where post-depositional effects may have locally been tectonically displaced and/or have altered the original Mn-bearing horizons.

The study took into account several items and was conducted through: (i) field observations, (ii) sampling for petrological analysis with Scanning Electron Microscope (SEM) examination of thin sections and (iii) ground geophysical surveys (magnetic and resistivity) along with profiles within 250 x 300 m^2 rectangle of the targeted area. The Mn bearing formation, NNE trending, outcrops over a 200 m long and 20-30 m wide. In the field, it is associated with and often grades into hornblende schist to the N-W and amphibolite to the S-E of Mankwadzi. It is dominantly composed of fine to medium grains of quartz, some of which are occasionally recrystallized and stretched (foliated or deformed) and mica. Dark bands, however, consist mostly of opaque Mn (?) oxide minerals that can be identified under a microscope. In some hand samples, veins and veinlets of similar opaque phases are also observed. But in many outcrops and hand samples, the host hornblende schist is macroscopically massive and sometimes strongly foliated. The main minerals examined under the microscope include quartz, feldspar, biotite and hornblende with occasional grains of pyrite and arsenopyrite. SEM images of Mn thin sections corroborate the distinctly banded to massive features observed both in hand samples and under the microscope. Individual bands often show variations in width and minerals density: garnet-rich bands alternate with garnet-poor layers in which sub-euhedral quartz or other silicate minerals may be present, with contacts in between fairly sharp. Mn-garnet usually occurs either in a matrix of dark, amorphous silica (chert) or in the garnetiferous bands. While the massive varieties of Mn rock often do not have visible banded areas and the garnet crystals of varying size appear to be cemented by silica (chert) and are distributed throughout the rock. The garnet exhibits, through semi-quantitative SEM analyses in banded and massive Mn rock, greater variability in Mn, Si, Al and Fe contents.

Regarding geophysical exploration through Reduced to Pole (RTP) data, obtained from the transformation of the Total Magnetic Intensity (TMI), the locations of observed Mn floats appear to fall on the flanks of the transformed maxima, suggesting that the inferred maximum RTP intensities may represent subsurface Mn ore in the area. A comparison of the apparent resistivity map with the analytic signal map suggests that the western anomalous zone depicted from the magnetic survey is also characterized by relatively low apparent resistivity values, suggesting that the zone is conductive. It strongly correlates, thus, with the Mn occurrence reported in this area. Additionally, the Mn outcrop in the Mankwadzi area exhibits a width and NE-trending extents enclosing hornblende schist, supported by interpretation from ground geophysical data. They reveal a NE-trending, highly magnetic but low resistivity main western zone with source depths >7 m roughly coinciding with the Mn occurrence. The shallow (<2.5 m), less persistent zone to the east, characterized by relatively high resistivity, appears to coincide with Mn floats in a dominantly lateritized zone. The Mn minerals, often associated with magnetic signatures, show paramagnetic and diamagnetic characteristics based on the ore oxidation state, thereby inducing positive and negative magnetic susceptibility values, respectively (Kropáček et al., 1975; Walid et al., 2013).

Manganese deposits in the Birimian of Ghana (e.g., Nsuta) or Burkina Faso (e.g., Tambao), exhibit several supergene-derived Mn oxide minerals such as cryptomelane, pyrolusite, psilomelane, nsutite and lithiophorite may be present in weathered lateritic or saprolitic horizons. They are overlying primary, mainly Mn, carbonate. The Mn oxide minerals of the study area seem to be the products of supergene alteration of primary Mn minerals in an underlying (protore) Mn.

Conclusions

The prospects for natural mineral resources in West Africa are high and are produced there from some of the largest and richest mineral deposits worldwide. The presence of such ore/mineral deposits suggests that others are likely to exist because the mineralization processes on explored formations commonly form clusters of mineral deposits. Mineral deposits are mainly associated with large-scale geological processes that occur in time and space. The magmas and hydrothermal fluids, fractures and faults, mountain ranges, and sedimentary basins are necessary for localizing mineral deposits.

In this volume, several new approaches were presented in various parts of the WAC and its surrounding areas for localizing mineralization by means of indirect or direct methods using geophysical and geochemical/geological field sampling for processing and laboratory analyses. The most significant results concern the detailed analyses of mineralization to extract information linked to their genesis and emplacement mechanisms in various geodynamic contexts. This mainly concerns the porphyry, VMS, sedex and lateritic sedimentary types. Mineral deposits do not occur randomly; their distribution is intimately linked to their geological history. The more we know about (i) the geology of each area of the WAC and (ii) the processes that control the regional and local distribution of mineral deposits, e.g., faulting systems, shears, stress regimes, host rock types, etc., the better we can know where new deposits will be found and what they will contain. In fact, such investigations could not be possible without the appropriate and cutting-edge tools on increasingly precise and targeted data (ICP-MS, Raman spectroscopy, high resolution geophysics and radiometric techniques, etc.)

The perspectives of knowledge of ore deposits could be targeted with artificial intelligence (e.g., fuzzy logic, neural networks, etc.) for a better approach to analyzing mineralization mechanisms (porphyry, metal-metalliferous, VMS, sedimentary and lateritic exhalative). This would help (i) localizing them through physical and chemical models, often used for analyses, but also (ii) forecasting and computing reserves.

A particular challenge for West Africa is the exploration of the hidden parts of the Precambrian WAC where they are covered by younger rocks, sand, and vegetation. The application of airborne geophysical surveys (e.g., magnetic, and radiometric) will be particularly important for exploration in these areas.

Younger sedimentary basins are also known to host a variety of mineral deposits rich in zinc, lead, phosphorous, aluminium, nickel, and titanium, as well as various industrial mineral products. However, these sedimentary basins are still largely under-explored.

Acknowledgements

I am grateful to all the geoscientists who accepted to peer-review the proposed articles to produce this special book dedicated to Prof. Th. Lasm. Their helpful suggestions and criticisms of the original manuscripts greatly improved the quality of the papers within this volume. I warmly thank all the referees some of whom peer-reviewed several articles, especially Richard England (University of Leicester, UK), Goodluck Anudu (University of Aberdeen, UK), Martin Lompo (Univ Ouagadougou, Burkina Faso), Sankar Bose (University of Kalkota, India), Fei Liu (Chinese Academy of Geological Sciences, Beijing, China), Simon Mitchell (University of the West Indies, Kingston, Jamaica), Luca Barale (Institute of Geosciences and Earth Resources, Torino, Italy), Qiang Yu (Chang'an University, China), Dick Tommy Claeson (Sveriges Geologiska Undersökning, Uppsala,, Sweden), Huan Cui (Vrije Universiteit Brussel, Belgium), Henri Masquelin (Universidad de la República, Montevideo, Uruguay), Salah A. Al-Khirbash (Sultan Qaboos University, Muscat, Oman), Israa S. Abu-Mahfouz (University of Oxford, UK), Mohammad Ismaiel (University of Hyderabad, India), Chokri Jallouli (King Saud University, Riyadh, Saudi Arabia), Dean Bullen (University of Portsmouth, UK), Lauren

Hoyer (University of KwaZulu-Natal, South Africa), Mohhamad Mehdi Farahpoor (Lorestan University, Iran), Sean C Johnson (University College, Dublin, Ireland), Abdelhak Boutaleb (FSTGAT-USTHB, Algiers, Algeria), Martin Stephen Griffin (Amec Foster Wheeler, Ashford, UK), Yacouba Coulibaly (Felix Houphouet-Boigny University of Cocody-Abidjan, Côte d'Ivoire), Saeed Alirezaei (Shahid Beheshti University, Iran), Athokpam K Singh (Wadia Institute of Himalayan Geology, Dehra Dun, India), Ali Ismail Aljubory (Mosul University, Iraq), Jinsen Zhang (Hebei University of Engineering, China), Bernard Bingen (Geological Survey of Norway, Trondheim, Norway), Bernhard Schulz (Technische Universitat Bergakademie Freiberg, Germany), Jean-Clair Duchesne (Université de Liège, Belgium), Stefan G. Mueller (University of Western Australia, Perth, Australia), Kaushik Das (Hiroshima University, Japan), Francesco Arboit (University of Dublin Trinity College, Ireland), Ismail Omer Yilmaz (Middle East Technical University, Ankara, Turkey), Amira El Tohamy (Nuclear Materials Authority, Cairo, Egypt), Mohammad Ebrahimi (University of Zanjan, Iran), Chandan Kumar Boraiaha (Central University of Kerala, India).

I also would like to express my special thanks (i) to Randell A. Stephenson (University of Aberdeen, UK), as editor of the GSL special publications, for his kind help during the procedures of peer-review and (ii) to the GSL Editorial staff, i.e. Bethan Phillips, Maggie Simmons, Tamzin Anderson and Rachael Kriefman for their support from handling, queries... to production of this volume. Finally, I especially thank Moussa Dabo (UCAD, Dakar, Senegal) for his involvement and contribution to IGCP 638 (UNESCO-IGCP program).

Figure captions

Fig. 1: (a) Map of the West African Craton (WAC) and surrounding areas with locations of studies presented in this special volume shown by red boxes. The dashed line shows the approximate modern shield margin of the WAC. The ages of the main formations are given in alphabetic order. **(b)** Compiled map of ore deposits in and around the WAC.

Fig. 2: Sketch of plate tectonic framework in which several major types of mineral deposits are formed. The main types (i to v) of ore deposits are shown (see Fig. 3 and described in the text).

Fig. 3: The main models of mineralization through the cross-section: **(a)** strato-volcano showing the relative locations of porphyry copper deposits, lead-zinc veins, gold-silver veins, and sulfur deposits; **(b)** metal-bearing hydrothermalism showing extensional tectonics between plates beneath the ocean; the metallic hydrothermal fluids reacting with the seawater to form mineral deposits; **(c)** volcanogenic massive sulfide (VMS) deposits. Hot hydrothermal fluids move along fractures in volcanic rocks towards the seabed and when these emerge and mix with cold ocean water, minerals of iron, copper, lead, and zinc sulfide can form on the seabed; **(d)** sediment-hosted (sedex) lead and zinc deposits. The fault is active during accumulation of sediments and mineral deposits and hydrothermal fluids move along the fault and fractures towards the seabed, minerals of iron, lead, and zinc sulfide are deposited and **(e)** soil profile in a laterite showing the progression of weathering effects on rock; aluminium and nickel are enriched by weathering.

References

Abdelsalam, M.G., Liegeois, J.P., Stern, R.J., 2002. The Saharan Metacraton. *Journal of African Earth Sciences*, 34, 119–136, https://doi.org/10.1016/S0899-5362(02)00013-1

Adissin Glodji, C.L., 2012. La zone de cisaillement de Kandi et le magmatisme associé dans la région de Savalou-Dassa (Bénin): étude structurale, pétrologique et géochronologique. *PhD thesis*, Université de Lyon, Lyon, France.

Ahmed, A.H., Arai, S., Abdel-Aziz, Y.M., Ikenne, M. and Rahimi, A., 2009. Platinum-group elements distribution and spinel composition in podiform chromitites and associated rocks from the upper mantle section of the Neoproterozoic Bou Azzer ophiolite, Anti-Atlas, Morocco. Journal of African Earth Sciences, 55, 92–104, https://doi.org/10.1016/j.jafrearsci.2009.02.005

Aïfa, T., 1993. Different styles of remagnetization in Devonian sediments from the north western Sahara (Algeria). *Geophysical Journal International*, 115, 529–537, https://doi.org/10.1111/j.1365-246X.1993.tb01204.x

Aïfa, T., Lefort, J.P., Ouddane, M., Calza, F., 1993. Mise en évidence d'antiformes générées en régime extensif sur la marge orientale du craton Ouest-Africain (région des Eglab): arguments paléomagnétiques et gravimétriques. *Bulletin du Service Géologique de l'Algérie*, 4, 121–136.

Aïfa, T. (Ed.), 2008. Investigations of Ore Deposits within the West African Craton and Surrounding Areas. *Journal of African Earth Sciences*, 50, 2-4, 55-272.

Aïfa, T., Lefort, J.P., Drareni, A., 2001. New paleopoles at 1.4–1.9 Ga from dyke swarms of the West African craton: paleomagnetic contribution to the accretionary phase of Rodinia. *Gondwana Research*, 4, 559–560, https://doi.org/10.1016/S1342-937X(05)70362-2

Aïfa, T. (Ed.), 2018. Paleoproterozoic Birimian Geology for Sustainable Development. *Journal of African Earth Sciences*, 148, 1-108.

Aïfa, T., Lo, K., 2020. Aeromagnetic modelling of Precambrian subsurface structures of the Tasiast area, NW Mauritania. *Geological Society*, *London*, *Special Publications*, **502**, https://doi.org/10.1144/SP502-2019-101

Aïfa, T., Merabet, N.E., 2020. Rock magnetic study on the Yetti-Eglab Intrusions, Sahara: contribution to the West African Craton geology. *Geological Society*, *London*, *Special Publications*, **502**, https://doi.org/10.1144/SP502-2019-198

Ait Hmeid, H., Akodad, M., Aalaoul, M., Baghour, M., Moumen, A., Skalli, A., Anjjar, A., Conti, P., Sfalanga, A., Ryazi Khyabani, F., Minucci, S., Daoudi, L., 2020. Clay mineralogy, chemical and geotechnical characterization of bentonite from Beni Bou Ifrour Massif (the Eastern Rif, Morocco). *Geological Society*, *London, Special Publications*, **502**, https://doi.org/10.1144/SP502-2019-25

Ajibade, A.C., Wright, J.B., 1989. The Togo–Benin– Nigeria Shield: evidence of crustal aggregation in the Pan-African belt. *Tectonophysics*, 165, 125–129, https://doi.org/10.1016/0040-1951(89)90041-3

Allek, K., Hamoudi, M., 2008. Regional-scale aeromagnetic survey of the south-west of Algeria: A tool for area selection for diamond exploration. *Journal African Earth Sciences*, 50(2-4), 67-78, https://doi.org/10.1016/j.jafrearsci.2007.09.018

Al-Juboury, A. (Eds.), 2018. Contributions to Mineralization. ISBN: 978-953-51-3749-8, Print ISBN: 978-953-51-3748-1, eBook (PDF) ISBN: 978-953-51-4068-9, https://doi.org/10.5772/intechopen.68760

Amadou, D.A., Konaté, M., Ahmed, Y., 2020. Geodynamic context of the Proterozoïc deposits of the Firgoun Region (eastern border of the West African Craton, West Niger). *Geological Society*, *London*, *Special Publications*, **502**, https://doi.org/10.1144/SP502-2019-115

Arndt, N.T., Lesher, C.M., Czamanske, G.K., 2005. Mantle-derived magmas and magmatic Ni-Cu-(PGE) deposits. *Economic Geology*, 100th Anniversary Volume, 5–23.

Asebriy, L., Cherkaoui, T.E., 1995. Tectonique cassante et sismotectonique dans le Rif et son avant-pays (Maroc). *Africa Geosciences Review*, 2, 141–149.

Augé, T., Joubert, M., Bailly, L., 2012. Typology of mafic-ultramafic complexes in Hoggar, Algeria: Implications for PGE, chromite and base-metal sulphide mineralisation. *Journal African Earth Sciences*, 63, 32-47.

Augustin, J., Gaboury, D., 2017. Paleoproterozoic plume-related basaltic rocks in the Mana gold district in western Burkina Faso, West Africa: implications for exploration and the source of gold in orogenic deposits. *Journal of African Earth Sciences*, 129, 17–30, https://doi.org/10.1016/j.jafrearsci.2016.12.007

Augustin, J., Gaboury, D., 2019. Multi-stage and multi-sourced fluid and gold in the formation of orogenic gold deposits in the world-class Mana district of Burkina Faso-Revealed by LA-ICP-MS analysis of pyrites and arsenopyrites. *Ore Geology Reviews*, 104, 495-521.

Ba, M.H., Jaffal, M., Lo, K., Youbi, N., Dahmada, M.E., Ibouh, H., Boumehdi, M.A., Aïfa, T., Amara, M., Jessell, M., Ernst, R.E., Bensalah, M.K., Söderlund, U., 2020. Mapping mafic dyke swarms, structural features, and hydrothermal alteration zones in Atar, Ahmeyim and Chami areas (Reguibat Shield, Northern Mauritania) using high-resolution aeromagnetic and gamma-ray spectrometry data. *Journal of African Earth Sciences*, 163, 103749.

Ballo, I., Hein, K.A.A., Guindo, B., Sanogo, L., Ouologuem, Y., Daou, G., Traore, A., 2016. The Syama and Tabakoroni goldfields, Mali. *Ore Geology Reviews*, 78, 578-585, https://doi.org/10.1016/j.oregeorev.2015.10.019

Baraou, I.S., Konaté, M., Ahmed, Y., Abdoul, W.D., 2018. Caractérisation de la déformation du socle de la zone mobile panafricaine du Sud Maradi, Sud Niger. *Afrique Science*, 14, 156–170.

Baraou, I.S., Konaté, M., 2020. New radiometric data from the South Maradi Pan-African formations, southern Niger. *Geological Society*, *London*, *Special Publications*, **502**, https://doi.org/10.1144/SP502-2019-151

Baratoux, L., Metelka, V., Naba, S., Jessell, M.W., Grégoire, M. Ganne, J., 2011. Juvenile Paleoproterozoic crust evolution during the Eburnean orogeny (~2.2–2.0 Ga), western Burkina Faso. *Precambrian Research*, 191, 18–45, https://doi.org/10.1016/j.precamres.2011.08.010

Barbarin, B., 1999. A review of the relationships between granitoid types, their origins and their geodynamic environments. *Lithos*, 46, 605-626.

Belkabir, A., Gibson, H.L., Marcoux, E., Lentz, D., Rziki, S., 2008. Geology and wall rock alteration at the Hercynian Draa Sfar Zn–Pb–Cu massive sulphide deposit, Morocco. *Ore Geology Review*, 33, 280–306, https://doi.org/10.1016/j.oregeorev.2007.03.001

Belkasmi, M., Ennih, N. (Eds.), 2010. 5th International 3MA Colloquium: Magmatism, Metamorphism, Associated Mineralizations. *Journal of African Earth Sciences*, 56, 2-3, 59-130.

Ben Aissi, L., El Boukhari, A., Hibti, M., Elharfi, M., Maacha, L., Zinbi, Y., 2005. Alteration hydrothermale et deformation ductile des roches volcaniques acides associées au gisement sulfuré de Draa Sfar (Jebilet Centrales, Maroc). *Estudios Geológicos*, 61, 147–160.
Ben Hamouda, B., Kemiha, M., Azzouz, N., 2017. Elimination of nitrates contained in leachate by adsorption on mixture bentonite-lime and on thermally chemically bentonite under microwave irradiation. [Elimination des nitrates contenus dans le lixiviat par adsorption sur un mélange bentonite-chaux et sur une bentonite activée thermiquement chimiquement sous irradiation micro-onde]. *Journal of New Sciences, Agriculture and Biotechnology*, 24, 2776-2783, E-ISSN 2286-5314
Bertrand-Sarfati, J., 1972. Stromatolites columnaires du Précambrien supérieur (Sahara nord-occidental): Inventaire, morphologie et microstructure des laminations. CNRS, *Thèse ès Sci*., Université Montpellier, 245p.
Bertrand-Sarfati, J., Moussine-Pouchkine, A., 1992. Formation et comblement d'une dépression intraplateforme engendrée par la croissance d'un biostrome stromatolitique, protérozoïque supérieur, Sahara algérien. *Comptes Rendus de l'Académie des Sciences, Paris*, 315, série II, 837–843.
Black, R., Caby, R., et al., 1979. Evidence for late Precambrian plate tectonics in West Africa. *Nature* (London), 278, 223–227, https://doi.org/10.1038/278223a0
Black, R., Liégeois, J.P., 1993. Cratons, mobile belts, alkaline rocks and continental lithospheric mantle: the Pan-African testimony. *Journal of the Geological Society*, London, 150, 89–98, https://doi.org/10.1144/gsjgs.150.1.0088
Blein O., T. Baudin, P. Chèvremont, A. Soulaimani, H. Admou, P. Gasquet, A. Cocherie, E. Egal, N. Youbi, P. Razin, M. Bouabdelli, P. Gombert. 2014. Geochronological constraints on the polycyclic magmatism in the Bou Azzer-El Graara inlier (Central Anti-Atlas Morocco). *Journal of African Earth Sciences*, 99, 287-306, https://doi.org/10.1016/j.jafrearsci.2014.04.021
Béziat, D., Dubois, M., Debat, P., Nikiéma, S., Salvi, S., Tollon, F., 2008. Gold metallogeny in the Birimian craton of Burkina Faso (West Africa). *Journal of African Earth Sciences*, 50, 215-233.
Blundell, D.J., Neubauer, F., von Quadt, A. (Eds.), 2002. The Timing and Location of Major Ore Deposits in an Evolving Orogen. *Geol. Soc. London*, Sp. Publications 204, 1-368, https://doi.org/10.1144/GSL.SP.2002.204.01.20
Bodinier, J., Dupuy, C. Dostal, J., 1984. Geochemistry of Precambrian ophiolite from Bou-Azzer, Morocco. *Contributions to Mineralogy and Petrology*, 87, 43–50, https://doi.org/10.1007/BF00371401
Bouabdellah, M., Fontboté, L., Haeberlin, Y., Llinares, L., Leach, D., Spangerberg, J., 1999. Zoned sulphur isotope signatures at the Mississippi Valley-type Touissit-Bou Beker-El Abed district (Morocco-Algeria)—Evidence for thermochemical sulphate reduction and mixing of sulfur sources, *in* Stanley, C.J., ed., Mineral deposits: processes to processing: Amsterdam, Balkema, 821–824.
Bouabdellah, M., Hibti, M., Maacha, L., Zouhair, M., Velasco, F., 2016. Geologic, Hydrothermal, and Geochemical Relationships Between Bimodal Magmatism and Massive Sulphide Mineralization in the Central Jebilet-Guemassa Province (Western Moroccan Hercynides). In *M. Bouabdellah and J.F. Slack (eds.)*, Mineral Deposits of North Africa, *Mineral Resource Reviews*, 437-459, https://doi.org/10.1007/978-3-319-31733-5_18, ISBN : 978-3-319-31731-1
Bouyo Houketchang, M., Toteu, S.F., Deloule, E., Penaye, J., Van Schmus, W.R., 2009. U-Pb and Sm-Nd dating of high-pressure granulites from Tchollíré and Banyo regions: Evidence for a Pan-African granulite facies metamorphism in north-central Cameroon. *Journal of African Earth Sciences*, 54, 144-154.
Caby, R., 1989. Precambrian terranes of Benin-Nigeria and northeast Brazil and the late Proterozoic South Atlantic fit. *Geological Society of America*, Special Papers, 230, 145–158.
Caby, R., Andreopoulos-Renaud, U., 1989. Age U–Pb a 620 Ma d'un pluton synorogénique de l'Adrar des Iforas (Mali). Conséquences pour l'âge de la phase majeure de l'orogène pan-africaine. *Comptes Rendus de l'Académie des Sciences*, Paris, 308, 307–314.
Caby, R., 2003. Terrane assembly and geodynamic evolution of Central-Western Hoggar: a synthesis. *Journal of African Earth Sciences*, 37, 133–159, https://doi.org/10.1016/j.jafrearsci.2003.05.003
Castaing, C., Triboulet, C., Feybesse, J.L., Chèvremont, P., 1993. Tectonometamorphic evolution Ghana, Togo and Benin in the light of Pan-African/Bresikiano orogeny. *Tectonophysis*, 218, 323–342, https://doi.org/10.1016/0040-1951(93)90322-B
Castaing, C., Bila, M., et al., 2003. Notice Explicative de la carte géologique et minière du Burkina Faso à 1/1000 000. 3ème edn.
Celli, N.L., S. Lebedev, A.J. Schaeffer, C. Gaina, 2020. African Cratonic Lithosphere Carved by Mantle Plumes. *Nature Communications*, 11(1), 92. https://doi.org/10.1038/s41467-019-13871-2
Chapman, R., Leake, B., Styles, M., 2002. Microchemical Characterization of Alluvial Gold Grains as an Exploration Tool. Gold Bulletin, 35, 53-65, https://doi.org/10.1007/BF03214838
Chapman, R., Leake, R.C., Bond, D.P.G., Stedra, V., Fairgrieve, B., 2009. Chemical and Mineralogical signatures of Gold Formed in Oxidizing Chloride Hydrothermal Systems and their Significance within

Populations of Placer Gold Grains Collected during Reconnaissance. *Economic Geology*, 104, 563–585, 0361-0128/09/3826/563-23

Chapman, R., Mileham, T., Allan, M., Mortensen, J., 2017. A distinctive Pd-Hg signature in detrital gold derived from alkalic Cu-Au porphyry systems. *Ore Geology Reviews*, 83, 84-102, https://doi.org/10.1016/j.oregeorev.2016.12.015

Chardon, D., 1997. Les déformations continentales archéennes : Exemple naturel et modélisation thermomécanique. *Thèse de doctorat*, l'Université de Rennes I. Mémoire de Géosciences-Rennes.

Chèvremont, P., Blein, O. et al. Anzar-Conseil, 2013. Notice explicative carte géol. Maroc (1/50 000), feuille Bou Azzer, Notes et Mémoires Serv. Géol. Maroc, N° 535 bis, MEM/BRGM. Carte géologique par Blein O., Chèvremont Ph., Razin, Ph., Baudin, T., Gasquet, D. (2013).

Ciampalini A., Garfagnoli F., Delventisette C., Moretti S., 2013. Potential Use of Remote Sensing Techniques for Exploration of Iron Deposits in Western Sahara and Southwest of Algeria. *Natural Resources Research*, 22(3), 179-190.

Chorlton, L.B., 2007. Generalized Geology of the World: Bedrock Domains and MajorFaults in GIS Format. *Geological Survey of Canada*, Open File 5529, 1 CD-ROM.

Choubert, G., 1952. Le volcan georgien de la région d'Alougoum (Anti-Atlas). *Comptes Rendus l'Académie des Sciences Paris*, 234, 350–352.

Clauer, N., Bonhomme, M., 1971. Preliminary Rb/Sr dating in the infracambrian near Atar (Mauritania). *European Colloquium of Geochronology*, Brussels, Abstracts, 1p.

Condie, K.C., 1992. Proterozoic Crustal Evolution, 1st ed., 10.Elsevier, eBook.

Condie, K.C., 2003. Supercontinents, superplumes and continental growth: the Neopropterozoic record. Geological Society, London, Special Publications, 206, 1–21, https://doi.org/10.1144/GSL.SP.2003.206.01.02

Condie, K.C., Des Marais, J.D., Abbott, D. 2000. Geological evidence for a mantle super plume event at 1.9 Ga. *Geochemistry, Geophysics, Geosystems*, 1, paper no. 2000GC000095, https://doi.org/10.1029/2000GC000095

Cook, N.J., Marshall, B. (Eds.), 2004. Metamorphic processes in ore formation and transformation. A thematic series of papers. *Ore Geology Reviews*, 24, 169-372.

Dabo, M., Aïfa, T., Miyouna, T., Abdoul Diallo, D., 2016. Gold mineralization paragenesis to tectonic structures in the Birimian of the eastern Dialé-Daléma Supergroup, Kédougou-Kéniéba Inlier, Senegal, West African Craton. *International Geology Review*, 58(7), 807-825.

Dada, S.S., Tubosun, I.A., Lancelot, J.R., Lar, A.U., 1993. Late Archean U–Pb age for the reactivated basement of Northeastern Nigeria. *Journal of African Earth Sciences*, 16, 405–412, https://doi.org/10.1016/0899-5362(93)90099-C

Daouda, Y.B., 1998. Lithostratigraphie et pétrologie des formations birimiennes de Toumodi-Fettêkro (Côte d'Ivoire): implication pour l'évolution crustale du Paléoprotérozoïque du Craton ouest africain. *PhD thesis*, Université d'Orléans, Orléans, France.

Davis, D.W., Hirdes, W., Schaltegger, E., Nunoo, E.A., 1994. U/Pb age constraints on deposition and provenance of Birimian and goldbearing Tarkwaian sediments in Ghana, West Africa. *Precambrian Research*, 67, 89-107.

Ddani, M., Meunier, A., Zahraoui, M., Beaufort, D., El Wartiti, M., Fontaine, C., Boukili, B., El Mahi, B., 2005. Clay mineralogy and chemical composition of bentonites from the Gourougou volcanic massif (northeast Morocco). *Clays and Clay Minerals*, 53, 250-267, https://doi.org/10.1346/CCMN.2005.0530305

Diène, M., Fullgraf, T., Diatta, F., Gloaguen, E., Gueye, M., Ndiaye, P.M., 2015. Review of the Senegalo-Malian shear zone system-Timing, kinematics and implications for possible Au mineralisation styles. *Journal of African Earth Sciences*, 112, 485-504. https://doi.org/10.1016/j.jafrearsci.2015.05.004

Dolansky, L.M., 2007. Controls on the genesis of hydrothermal cobalt mineralisation: insights from the mineralogy and geochemistry of the Bou Azzer deposits, Morocco. *Unpublished Master thesis*, McGill University, Montreal, Canada, 162p.

Doumbia, S., Pouclet, A., Kouamelan, A., Peucat, J.J., Vidal, M., Delor, C., 1998. Petrogenesis of juveniletype Birimian (Paleoproterozoic) granitoids in central Côte-d'Ivoire West Africa: geochemistry and geochronology. Precambrian Research, 87, 33–63, https://doi.org/10.1016/S0301-9268(97)00201-5

dos Santos, T.J.S., Fetter, A.H., Neto, J.A.N., 2008. Comparisons between the northwestern Borborema Province, NE Brazil, and the southwestern Pharusian Dahomey Belt, SW Central Africa. *Geological Society*, London, Special Publications, 294, 101–120, https://doi.org/10.1144/SP294.6

Drareni, A., Peucat, J.J., Fabre, J. 1995. Isotopic data (Sr, Nd, Pb) from the W African Craton: the «Dorsale Reguibat», the Eglab massif (Algeria). *Terra Abstracts*, 47, 102.

Driouch, Y., Belkasmi, M., Ennih, N., 2010. Special issue on magmatism, metamorphism, associated mineralizations, Fez, Morocco: Selected papers. *Journal of African Earth Sciences*, 56, 96-126. https://doi.org/10.1016/j.jafrearsci.2009.05.013

Dubroeucq, D., Geissert, D., Quantin, P., 1998. Weathering and soil-forming processes under semi-arid conditions in two Mexican volcanic ash soils. *Geoderma*, 86, 99–122, https://doi.org/10.1016/S0016-7061(98)00033-0

Ebot, V., Neba, G., Suh, E., 2016. Environmental geochemistry of mine tailings soils in the artisanal gold mining district of Bétaré–Oya, Cameroon. *Geochemistry Exploration Environment Analysis*, 6, 52–62.

El Basbas, A., M. Aissa, H. Ouguir, My L. Mahdoudi, A. Madi, M. Zouhair, 2020. Ouansimi Copper Mineralization (Western Anti-Atlas, Morocco): Paragenetic Sequence and Circulation of Gangue Hosted Paleofluids. *Journal of African Earth Sciences*, 162, 103692.

El Boukhari, A., Chabane, A., Rocci, G. Tane, J.-L., 1992. Upper proterozoic ophiolites of the Siroua Massif (anti-atlas, Morocco) a marginal sea and transform fault system. *Journal of African Earth Sciences*, 14, 67–80, https://doi.org/10.1016/0899-5362(92)90056-I

El Rhazi, M., Hayashi, K.I. 2002. Mineralogy, geochemistry, and age constraints on the Beni Bou Ifrour skarn type magnetite deposit, Northeastern Morocco. *Resource Geology*, 52, 25-39, https://doi.org/10.1111/j.1751-3928.2002.tb00114.x

Els, G., Eriksson, P. (Eds.), 2006. Placer Formation and Placer Minerals. *Ore Geology Reviews*, 28, 1-548.

En-Naciri, A., 1995. Contribution à l'étude du district à Co, As, (Ni, Au, Ag) de Bou Azzer, Anti Atlas (Maroc), données minéralogiques et géochimiques; étude des inclusions fluides. *Unpublished PhD thesis*, Université d'Orléans, France, 238p.

En-Naciri, A., Barbanson, L., Touray, J.C., 1995. Mineralised hydrothermal solution cavities in the Co-As Aït Ahmane mine (Bou Azzer, Morocco). *Mineralium Deposita*, 30, 57–77.

Ennih, N., Liégeois, J.P., Thomas, B. (Eds.), 2004. Key Points on African Geology. *Journal of African Earth Sciences*, 39, 3-5, 91-570.

Ennih, N., Liégeois, J.P., (Eds.), 2008. The Boundaries of the West African Craton. *Geological Society*, London, Special Publications, 297, NP, 1 January 2008, https://doi.org/10.1144/SP297.0

Essaifi, A., Goodenough, K., Tornos, F., Outigua, A., Ouadjou, A., Maacha, L., 2019. The Moroccan Massive Sulphide Deposits: Evidence for a Polyphase Mineralization. *Minerals*, 9, 156, https://doi.org/10.3390/min9030156

Essaraj, S., Boiron, M.-C., Cathelineau, M., Banks, D.A., Benharref, M., 2005. Penetration of surface-evaporated brines into the Proterozoic basement and deposition of Co and Ag at Bou Azzer (Morocco): evidence from fluid inclusions. *Journal of African Earth Sciences*, 41, 25–39, https://doi.org/10.1016/j.jafrearsci.2005.03.001

Ferré, E.C., Gleizes, G., Caby, R., 2002. Obliquely convergent tectonics and granite emplacement in the Trans-Saharan belt of Eastern Nigeria: a synthesis. *Precambrian Research*, 114, 199–219, https://doi.org/10.1016/S0301-9268(01)00226-1

Fon, A.N., Che, V.B., Suh, C.E., 2012. Application of electrical resistivity and chargeability data on a GIS platform in delineating auriferous structures in a deeply weathered lateritic terrain, eastern Cameroon. *International Journal of Geosciences*, 3, 960–971, https://doi.org/10.4236/ijg.2012.325097

Franceschinis, P.R., Rapalini, A.E., Sánchez Bettucci, L., Martínez Dopico, C., Milanese, F.N., 2019. Paleomagnetic confirmation of the 'unorthodox' configuration of Atlantica between 2.1–2.0 Ga. *Precambrian Research*, 334, 105447, https://doi.org/10.1016/j.precamres.2019.105447

Franklin, J.M., 1993. Volcanic associated massive sulfide deposits, *in* Kirkham, R.V., inclair, W.D., Thorpe, R.I., and Duke, J.M. (Eds.), Mineral deposit modeling: *Geological Association of Canada* Special Paper 40, p315–334.

Franklin, J.M., 1996. Volcanic-associated massive sulphide base metal. In: Ekstrand, O.R., Sinclair, W.D. and Thorpe, R.I. (eds) Canadian Mineral Deposit Types. *Geological Survey of Canada*, Special Publications, 8, 158–183.

Freyssinet, P.H., Lecomte, P., Edimo, A., 1989. Dispersion of gold and base metals in the Mborguene lateritic profile, East Cameroon. *Journal of Geochemical Exploratio*n, 32, 99–116, https://doi.org/10.1016/0375-6742(89)90050-2

Freyssinet, Ph, Butt, C.R.M., Morris, R.C., Piantone, P., 2005. Ore-forming processes related to lateritic weathering. *Economic Geology*, 100th Anniversary Volume, p. 681–722.

Frost, B.R., Barnes, C.G., Collins, W.J., Arculus, R.J., Ellis, D.J., Frost C.D., 2001. A geochemical classification for granitic rocks. *Journal of Petrolog*y, 42(11), 2033-2048.

Gaboury, D., Pearson, V., 2008. Rhyolite geochemical signatures and association with volcanogenic massive sulfide deposits: examples from the Abitibi Belt, Canada. *Economic Geology*, 103, 1531–1562, https://doi.org/10.2113/gsecongeo.103.7.1531

Ganwa, A., Frisch, W., Siebel, W., Shang, K.C., Ondoa, M.J., Satir, M., Numbem, T.J., 2008. Zircon 207Pb/206Pb evaporation ages of Panafrican metasedimentary rocks in the Kombé-II area (Bafia Group, Cameroun): constraints on protolith age and provenance. *Journal of African Earth Sciences*, 51, 77–88, https://doi.org/10.1016/j.jafrearsci.2007.12.003

Ganwa, A.A., Siebel, W., Frisch, W., Shang, C.K., 2011. Geochemistry of magmatic rocks and time constraints on deformational phases and shear zone slip in the Meïganga area, central Cameroon. *International Geology Review*, 53, 759–784.

Giorgis, I., Bonetto, S., Giustetto, R., Lawane, A., Pantet, A., Rossetti, P., Thomassin, J.H., Vinai, R., 2014. The lateritic profile of Balkouin, Burkina Faso: Geochemistry, mineralogy and genesis. Journal of African Earth Sciences, 90, 31-48, https://doi.org/10.1016/j.jafrearsci.2013.11.006

Gnanzou, A., 2006. Etude lithostratigraphique de la région de Hiré dans le centre-sud de la Côte d'Ivoire (Permis de recherche PRA 37): implication à la connaissance de la minéralisation aurifère. *DEA*, UFR STRM, University of Cocody, Abidjan, Ivory Coast.

Goodfellow, W.D., Lydon, J.W., Turner, R.J.W., 1993. Geology and genesis of stratiform sedimenthosted (SEDEX) zinc-lead-silver sulphide deposits. *Mineral Deposit Modeling* (Kirkham, R.V., Sinclair, W.D., Thorpe, R.I., Duke, J.M .(Eds.), *Geol. Assoc. Canada*, Spec. Paper 40, 201–251.

Hamilton, J. M., Bishop, D. T., Morris, H.Gouedji, F., Picard, C., et al., 2014. The Samapleu mafic– ultramafic intrusion and its Ni–Cu-PGE mineralization: an Eburnean (2.09 Ga) feeder dyke to the Yacouba Layered Complex (Man Archean craton. Western Ivory Coast). *Bulletin de la Société géologique de France*, 185, 393–411, https://doi.org/10.2113/gssgfbull.185.6.393

Gouedji, G.E.F., Audet, M.-A., Coulibaly, Y., Picard, C., Ouattara, N., Bakayoko, B., 2018. Apport de la minéralogie et de la cristallochimie à la connaissance des conditions de mise en place de l'intrusion mafique-ultramafique à Ni–Cu-EGP de Samapleu (complexe lité Yacouba, ouest de la Côte d'Ivoire). *Revue africain et malgache de recherches scientifiques*, 06, 49–67.

Gouedji, F., Picard, C., Audet, M.A., Goncalvès, P ., Coulibaly, Y., Bakayoko, B., 2020. The Samapleu mafic-ultramafic intrusion (western Ivory Coast): cumulate of a high-Mg basaltic magma with (coeval) ultrahigh-temperature-medium-pressure metamorphism. *Geological Society, London, Special Publications*, **502**, https://doi.org/10.1144/SP502-2019-130

Gunn, P.J., Maidment, D., Milligan, P.R., 1997. Interpreting aeromagnetic data in areas of limited outcrop. *AGSO Journal of Australian Geology & Geophysics*, 17, 175–185.

Haldar, S.K., 2020. Introduction to Mineralogy and Petrology, 436p., Elsevier, ISBN :978-0-12-820585-3, https://doi.org/10.1016/C2019-0-00625-5

Halls, H.C., Campal, N., Davis, D.W., Bossi, J., 2001. Magnetic studies and U–Pb geochronology of the Uruguayan dyke swarm, Rio de la Plata craton, Uruguay: paleomagnetic and economic implications. *Journal of South American Earth Sciences*, 14, 349–361, https://doi.org/10.1016/S0895-9811(01)00031-1

Hallarou, M.M., Konaté, M., Olatunji, A.S., Ahmed, Y., 2020a. The Paleoproterozoic porphyry copper-molybdenum deposit of Kourki (Liptako Province, western Niger). *Geological Society, London, Special Publications*, **502**, https://doi.org/10.1144/SP502-2019-139

Hallarou, M.M., Konate, M., Olatunji, A.S., Ahmed, Y., Ajayi, F.F., Abdul, R.M. 2020b. Re-Os ages for the Kourki porphyry Cu-Mo deposits, north west Niger (West Africa): geodynamic implications. *European Journal of Environment and Earth Sciences*, 1, 1-13, https://doi.org/10.24018/ejgeo.2020.1.4.43

Hammerbeck, E.C.I., Schurmann, L.W., 1998. Nickel, *in* Wilson, M.G.C., and Anhaeusser, C.R. (Eds.), 1998, The mineral resources of South Africa: Handbook, Council for Geoscience, 16, p. 471–482.

Hassenforder, B. 1987. La Tectonique Panafricaine et Varisque de l'Anti-Atlas dans le Massif du Kerdous (Maroc). *Thèse de doctorat Es-Sciences*, Université de Strasbourg, 220p.

Hein, K.A.A., Tshibubudze, A. 2016. Manganese deposits of the Oudalan province in the northeast of Burkina Faso, and Ansongo Inlier in eastern Mali. *Ore Geology Reviews*. https://doi.org/10.1016/j.oregeorev.2015.11.008

Hein, K.A.A., 2016. The Bagassi gold deposits on the eastern margin of the Houndé greenstone belt, Burkina Faso, Ore Geology Reviews. https://doi.org/10.1016/j.oregeorev.2015.10.028

Helmstaedt, H.H., Scott, D.J., 1992. The Proterozoic ophiolite problem. In: Condie, K.C. (Ed.) Proterozoic Crustal Evolution, 1st ed., 10, Chapter 2, 55–95. Elsevier, eBook.

Hibti, M., 2001. Les amas sulfurés des Guemassa et des Jebilet (Meseta Sud-Occidentale, Maroc): Témoins de l'hydrothermalisme précoce dans le bassin mesetien. *PhD thesis*, Marrakech University, Morocco.

Higashihara, M., Marutani, M., Bellal, A.O., Dioumassi, B., Ousmane, D., Emenetoullah, L., 2004. Platetectonic and metallogenic evolutions of western Reguibat shield: proposition of a hypothesis. Prog. Abstr. *Internat. Geol. Correlation Prog. Conf. 485* (UNESCO/IUGS), Nouakchott, 5–13 Dec. 10–13.

Hodel, F., Macouin, M. et al., 2017. Unusual massive magnetite veins and highly altered Cr-spinels as relics of a Cl-rich acidic hydrothermal event in Neoproterozoic serpentinites (Bou Azzer ophiolite, Anti-Atlas, Morocco). *Precambrian Research*, 300, 151–167, https://doi.org/10.1016/j.precamres.2017.08.005

Holler, W. and Ghandi, S.M. 1995. Silver-bearing sulfosalts from the metamorphosed Rampura–Agucha Zn–Pb–(Ag) deposit, Rajasthan, India. *Canadian Mineralogy*, 33, 1047–1057.

Houssou, N.N., 2013. Etude pétrologique, structurale et métallogénique du gisement aurifère d'Agbahou, Divo, Côte d'Ivoire. *PhD Thesis*, Université Félix Houphouët-Boigny, Abidjan, Côte d'Ivoire.

Houssou, N.N., Allialy, M.E., Kouadio, F.J.L.-H., Gnanzou, A., 2017. Structural control of auriferous mineralisation in the Birimian: case of the Agbahou deposit in the region of Divo, Côte d'Ivoire. *International Journal of Geoscience*, 8, 189–204, https://doi.org/10.4236/ijg.2017.82008

Ikenne, M., Madi, A., Gasquet, D., Cheilletz, A., Hilal, R., Mortaji, A., Mhaili, E., 2005. Petrogenetic significance of podiform chromitite from the neoproterozoic ophiolitic complex of Bou Azzer – Anti-Atlas Morocco. *Africa Geoscience Review*, 13, 131–148.

Ikenne, M., Souhassou, M., Saintilan, N.J., Karfal, A., Hassani, A. E. L., Moundi, Y., Ousbih, M., Ezzghoudi, M., Zouhir, M., Maacha, L., 2020. Cobalt-nickel-copper arsenide, sulfarsenide and sulfide mineralization in the Bou Azzer window, Anti-Atlas, Morocco: one century of multi-disciplinary and geological investigations, mineral exploration and mining. *Geological Society, London, Special Publications*, **502**, , https://doi.org/10.1144/SP502-2019-132

Ilboudo, H., Wenmenga, U., Sawadogo, S., Toufik, R., 2017. Mise en évidence d'un assemblage à disthène–staurotide–grenat dans le secteur de Mangodara, ceinture de Banfora, Burkina Faso, Afrique de l'Ouest: implication dans la genèse des gîtes minéraux polymétalliques. Afrique Sciences, 13, 220–231.

Ilboudo, H., Sawadogo, S., Ouiya, P., Hien, A., Yaméogo, F.H. 2019. Géologie des minéralisations (Au) en veines de Mouro dans le système Birimien de Banfora, Burkina Faso – Afrique de l'Ouest: approche gitologique par exploitation d'un site d'orpaillage. *Afrique Science*, 15, 92–104

Ilboudo, H., Sawadogo, S., Zongo, G.H., Naba, S., Wenmenga, U., Lompo, M., 2020. Geochemistry and geodynamic constraint of volcanic and plutonic magmatism within the Banfora Belt (Burkina-Faso, West-Africa): contribution to mineral exploration. *Geological Society, London, Special Publications*, **502**, https://doi.org/10.1144/SP502-2019-86

Inglethorpe, S.D.J., Morgan, D.J., Highley, D.E., Bloodworth, A., 1993. British Geological Survey:industrial minerals laboratory manual. *Journal of Mathematics*, 124.

Jaffal, M., El Goumi, N., Kchikach, A., Aïfa, T., Khattach, D., Manar, A., 2010. Gravity and magnetic investigations in the Haouz basin, Morocco. Interpretation and mining implications. *Journal of African Earth Sciences*, 58, 331-340, https://doi.org/10.1016/j.jafrearsci.2010.03.012

Jefferson, C.W., Delaney, G. (Eds.), 2007. ExtechIV: Geology and Uranium Exploration TECHnology of the Proterozoic Athabasca Basin, Saskatchewan and Alberta. Geol. Assoc. of Canada Mineral Deposits sp. Publ. 4, Saskatchewan Geol. Soc. Sp. Publ. 18, *Geol. Surv. of Canada Bulletin*, 588, 644p.

Jessell, M., Liégeois, J.-P. (Eds.), 2015. Tectonics, mineralisation and regolith evolution of the West African Craton. *Journal of African Earth Sciences*, 112, Part B, 377-610. 100 years of research on the West African Craton

Jessell, M.W., Cawood, P.A., Miller, J.M., 2016. Editorial: Craton to Regional-scale analysis of the Birimian of West Africa. *Precambrian Research*. https://doi.org/10.1016/j.precamres.2015.12.014

Johnson, S.P., Thorne, A.M., Tyler, I.M., Korsch, R.J., Kennett, B.L.N., Cutten, H.N., Goodwin, J., Blay, O., Blewett, R.S., Joly, A., Dentith, M.C., Aitken, A.R.A., Holzschuh, J., Salmon, M., Reading, A. , Heinson, G., Boren, G., Ross, J., Costelloe, R.D., Fomin, T., 2013. Crustal architecture of the Capricorn Orogen, Western Australia and associated metallogeny. *Australian Journal of Earth Sciences: An International Geoscience Journal of the Geological Society of Australia*, 60:6-7, 681-705, https://doi.org/10.1080/08120099.2013.826735

Kahoui, M., Drarenl, A., Fabre, J., Peucat, J.J., Kaddour, M., 1996. Age éburnéen du complexe alcalin du complexe annulaire alcalin du Djebel Drissa (Est de la Dorsale Réguibat, Algérie). Mémoires du Service Géologique de l'Algérie, 8, 15–22.

Kahoui, M., Mahdjoub, Y., 2004. An Eburnian alkaline–peralkaline magmatism in the Reguibat rise: the Djebel Drissa ring complex (Eglab Shield, Algeria). *Journal of African Earth Sciences*, 39, 115–122, https://doi.org/10.1016/j.jafrearsci.2004.07.057

Kahoui, M., Mahdjoub, Y., Kaminsky, F.V., 2008. Possible primary sources of diamond in the North African diamondiferous province. Geological Society, London, Special Publications, 297, 77–109, https://doi.org/10.1144/SP297.5

Kahoui, M., Kaminsky, F.V., Griffin, W.L., Belousova, E., Mahdjoub, Y., Chabane, M., 2012. Detrital pyrope garnets from the El Kseibat area, Algeria: a glimpse into the lithospheric mantle beneath the north-eastern edge of the West African Craton. Journal of African Earth Sciences, 63, 1–11, https://doi.org/10.1016/j.jafrearsci.2011.10.005

Kahoui, M., Mahdjoub, Y., 2004. An Eburnean alkaline-peralkaline magmatism in the Reguibat Rise: the Djebel Drissa ring complex (Eglab shield, Algeria). *Journal of African Earth Sciences*, 39, 115–122.

Kankeu, B., Greiling, R.O., Nzenti, J.P., 2009. Pan-African strike-slip tectonics in eastern Cameroon-Magnetic fabrics (AMS) and structure in the Lom basin and its basement. *Precambrian Research*, 174, 258–272, https://doi.org/10.1016/j.precamres.2009.08.001

Kankeu, B., Greiling, R.O., Nzenti, J.P., Basahak, J., Hell, J.V., 2012. Strain partitioning along the Neoproterozoic Central Africa Shear zone system: structures and magnetic fabrics (AMS) from Meiganga area, Cameroun. *Neues Jahrbuch fur Geologie und Palaeontologie Abhandlungen*, 265, 27–48, https://doi.org/10.1127/0077-7749/2012/0244

Kemp, A.I.S., Hawkesworth, C.J., 2003. Granitic perspectives on the generation and secular evolution of the continental crust. In: Rudnick R.L. (Ed.), The crust. *Treatise in Geochemistry*, 3, 349-410.

Kious, W.J., Tilling, R.I., 1996, This dynamic Earth: The story of plate tectonics. Accessed January 4, 2021, at http://pubs.usgs.gov/publications/text/dynamic.html#anchor19309449.

Kolb, J., Petrov, N., 2016. The Guelb Moghrein Cu-Au deposit: Neoarchaean hydrothermal sulfide mineralization in carbonate-facies iron formation. *Ore Geology Reviews*, 78, 573-577. https://doi.org/10.1016/j.oregeorev.2015.09.003

Konaté, M., Ahmed, Y., et al., 2018. U–Pb detrital zircon ages of sediments from the Firgoun and Niamey areas (eastern border of West African Craton, West Niger). *Comptes Rendus Géoscience*, 350, 267–278, https://doi.org/10.1016/j.crte.2018.06.005

Kouyaté, D., Söderlund, U., et al., 2013. U–Pb baddeleyite and zircon ages of 2040 Ma, 1650 Ma and 885 Ma on dolerites in the West African Craton (Anti-Atlas inliers): possible links to break-up of Precambrian supercontinents. *Lithos*, 174, 71–84, https://doi.org/10.1016/j.lithos.2012.04.028

Kropá c ek, V., Krs, M., Bucha, V. 1975. Magnetic properties of natural Mn-oxides. *Studies in Geophysics and Geodynamics*, 19, 261–274, https://doi.org/10.1007/BF01614255

Kwékam, M., Affaton, P., Bruguier, O., Liégeois, J-P., Hartmann, G., Njonfang, E., 2013. The Pan-African Kekem gabbro-norite (West-Cameroon), U-Pb zircon age, geochemistry and Sr-Nd isotopes: Geodynamical implication for the evolution of the Central African fold belt. *Journal of African Earth Sciences*, 84, 70-88.

Kwékam, M., Hartmann, G., Njanko, T., Tcheumenak, K.J., Fozing, E.M., Njonfang, E., 2015. Geochemical and isotope Sr-Nd character of Dschang biotite granite: implications for the pan-African continental crust evolution in West-Cameroon (Central Africa). *Earth Sciences Research*, 4(1), 88-102.

Kwékam, M., Dunkl, I., Fozing, E.M., Hartmann, G., Njanko , T., Tcheumenak, K.J., Njonfang, E., 2020. Syn-kinematic ferroan high-K I-type granites from Dschang in southwestern Cameroon: U-Pb age, geochemistry and implications for crustal growth in the late Pan-African Orogeny. *Geological Society, London, Special Publications*, **502**, https://doi.org/10.1144/SP502-2019-19

Leach, D.L., Sangster, D.F., Kelley, K.D., Large, R.R., Garven, G., Allen, C.R., Gutzmer, J., Walters, S., 2005, Sediment-hosted lead-zinc deposits: A global perspective: *Economic Geology*,100th Anniversary Volume, p. 61–608.

Leaman, P., and Staude, J.-M., 2002 Metallogenic evolution of the western Tethys of Turkey and Iran, *in* Metal Mining Agency of Japan, Presentation from forum on mineral potential of Asia: Mineral Resource Information Center, 42p., CD ROM.

Lebedev, V.I.B., Orovikov, A.A., Borisenko, A.S., Azizi, R., Ishkov, Y.M., Borisenko, D.A., 1999. Physicochemical constraints of cobalt ore formation in the Bou Azzer deposit, Morocco. *Doklady Earth Sciences*, 368, 985–998.

Leblanc, M., 1981. Ophiolites précambriennes et gîtes arséniés de cobalt (Bou Azzer-Maroc). *Notes et Mémoiresdu Service Géologique*, Maroc, 280, 360.

Leblanc, M., Lbouabi, M., 1988. Native silver mineralisation along a rodingite tectonic contact between serpentinite and quartz diorite (Bou Azzer, Morocco). *Economic Geology*, 83, 1379–1391, https://doi.org/10.2113/gsecongeo.83.7.1379

Lefort, J.P., Aïfa, T., Ouddane, M., 1994. Modélisation magnétique des filons subméridiens de l'ensemble Yetti–Eglab (Dorsale Réguibat): conséquences géodynamiques concernant la marge orientale du craton ouest-africain. *Bulletin du Service Géologique de l'Algérie*, 5, 129–149.

Lefort, J.P., Aïfa, T., 2001. Paleomagnetic and geochronological evidence for a large rotation of the West African craton between 1.9 and 1.4 Ga: a kinematic model for the fragmentation of Columbia and the accretion of Rodinia. *Gondwana Research*, 4, 678–679, https://doi.org/10.1016/S1342-937X(05)70474-3

Lefort, J.P., Aïfa, T., 2002. Evidence for a circumterrestrial loop of the APWP of the West African Craton between 2.2 and 0.9 Ga: its temporary amalgamation to Columbia and Rodinia. *11th Quadrennial IAGOD Symposium and Geocongress 2002, Sedimentary, Magmatic and Ore-forming Responses to Compressional and Tensional Tectonics: A Focus on Africa*, Windhoek, Namibia, 22–27 July 2002, 32.

Lefort, J.P., Aïfa, T., Bourrouilh, R., 2004. Evidences paléomagnétiques et paléontologiques en faveur d'une position antipodale du Craton ouest africain et de la Chine du Nord dans le supercontinent Rodinia: conséquences paléogéographiques. *Comptes Rendus de Geosciences*, 336, 159–165, https://doi.org/10.1016/j.crte.2003.11.003

Léger, J.M., Liègeois, J.P., Pouclet, A. Vicat, J.P., 1992. Occurrence of syntectonic alkali-pyroxene granites of Eburnean age (2.1 Ga) in Western Niger. Abstracts, *14ème Réunion Annuelle des Sciences de la Terre*, Toulouse, France. *Société Géologique de France*, 96.

Lemoine, S., 1988. Evolution géologique de la région de Dabakala (Nord-Est de la Côte d'Ivoire) au Protérozoïque Inférieur. *PhD thesis*, Université Clermont- Ferrand, Clermont-Auvergne, France.

Lemoine, S., Tempier, P., Bassot, J.P., Caen-Vachette, M., Vialette, Y., Toure, S., Wenmenga, U., 1990. The Burkinian orogenic cycle, precursor of the Eburnian Orogeny in West Africa. *Geology Journal*, 25, 171–188, https://doi.org/10.1002/gj.3350250208

Levresse, G., 2001. Contribution à l'établissement d'un modèle génétique des gisements d'Imiter (Ag-Hg), Bou Madine (Pb-Zn-Cu-Ag-Au) et Bou Azzer (Co-Ni-As-Ag-Au) dans l'Anti-Atlas marocain. *Unpublished PhD thesis*, CRPG-CNRS, Nancy, France, 191p.

Li, X.F., 2001. Deformation-metamorphism and gold mineralization in ductile shear zone. *Journal of the Gulin Institute of Technology*, 3, 207–212.

Liégeois, J.P., Latouche, L., Boughrara, M., Navez, J., Guiraud, M., 2003. The LATEA metacraton. (Central Hoggar, Tuareg shield, Algeria): behaviour of an old passive margin during the Pan-African orogeny. *Journal of African Earth Sciences*, 37, 161–190, https://doi.org/10.1016/j.jafrearsci.2003.05.004

Lydon, J.W., 1988. Volcanogenic massive sulphide deposits part 1: A descriptive model, *in* Roberts, R.G. and Sheahan, P.A., Eds., Ore deposit models: *Geoscience Canada Reprint Series* 3, 145–153.

Lydon, J.W., 1996. Sedimentary exhalative sulphides (sedex), *in* Eckstrand, O.R., Sinclair, W.D., and Thorpe, R.I., eds., Geology of Canadian mineral deposit types. *Geological Survey of Canada*, Geology of Canada, no. 8, 130–152.

Maacha, L. 1994. Etude géologique et métallogénique des gisements cobaltifères de Bou Azzer-Centre (Anti-Atlas, Maroc). Mém. C.E.A, Univ. Marrakech, 119.

Maacha, L., Azizi-Samir, R. Bouchta, R., 1998. Gisements cobaltifères du district de Bou Azzer (Anti-Atlas): structure, minéralogie et conditions de genèse. *Chronique de la Recherche Minière*, 531/532, 65–75.

Maacha, L., 2013. Etude métallogénique et géophysique des minéralisations cobaltifères et cuprifères de la boutonnière de Bou Azzer. Anti-Atlas. Maroc. *Thèse Doctorat D'état*, University Caddi Ayyad – Marrakech, 304p.

Maacha, L., Elghorfi, M., En-Naciri, A., Sadiqqi, O, Soulaimani, A., Alansari, A., Bhilisse, M., 2015. Nouvelles données isotopiques et d'inclusions fluides des minéralisations cobaltifères de Bou Azzer. Apport à la géologie économique de la boutonnière. (Anti-Atlas central, Maroc). *Notes et Mémoires du Service Géologique*, Maroc, 579, 133–139.

Mahdjoub, Y., Drareni, A., Gani, R., 1994. Accrétion crustale et tectonique verticale à l'Eburnéen dans les massifs des Eglab et du Yetti (Dorsale Réguibat, Algérie). *Bulletin du Service Géologique de l'Algérie*, 5, 97–107.

Maier, W.D., 2005. Platinium-group element (PGE) deposits and occurrences: mineralization styles, genetic concepts, and exploration criteria. *Journal of African Earth Sciences*, 41, 165-191.

McLaurin, N., White, N., Ashton, J. (Eds.), 2005. Geodynamics and ore deposit evolution in Europe. *Ore Geology Reviews*, 27, 1-350.

Marcoux, E., Belkabir, A., Gibson, H.L., Lentz, D., Ruffet, G., 2008. Draa Sfar, Morocco: a Visean (331 Ma) pyrrhotite-rich, polymetallic volcanogenic massive sulphide deposit in a Hercynian sedimentdominant terrane. *Ore Geology Review*, 33, 307–328, https://doi.org/10.1016/j.oregeorev.2007.03.004

Markwitz, W., Hein, K.A.A., Miller, J., 2016. Compilation of West African mineral deposits: Spatial distribution and mineral endowment. *Precambrian Research*, 274, 61-81, https://doi.org/10.1016/j.precamres.2015.05.028

Marutani, M., Higashihara, M., Watanabe, Y., Murakami, H., Kojima, G., Dioumassi, B., 2005. Metallic ore deposits in the Islamic Republic of Mauritania: Shigen- Chishitsu. *The Society of Resource Geology*, 55, 59–70.

Masquelin, H., Aïfa, T., Scaglia, F., Basei, M.A.S., 2021. The Archean Pavas Block in Uruguay: extension and tectonic evolution based on LA-ICP-MS U-Pb ages and airborne geophysics. *Journal of South American Earth Sciences*, minor revision, revised.

Masurel, Q., Thébaud, N., Miller, J.M., Urlich, S., 2017. The tectono-magmatic framework to gold mineralisation in the Sadiola-Yatela gold camp and implications for the paleotectonic setting of the Kédougou-Kénieba inlier, West Africa. *Precambrian Research*, 292, 35-56. https://doi.org/10.1016/j.precamres.2017.01.017

McQueen, K.G., 2005. Ore deposit types and their primary expressions. In C.R.M. Butt, I.D.M. Robertson, K.M. Scott, M. Cornelius (Eds.), Regolith Expression of Australian Ore Systems, 1-14, chapter 1, 1st Edition, CRC LEME, Bentley, WA

Merabet, N.E., Mahdjoub, Y., Kahoui, M., Maouche, S., Abtout, A., Henry, B., Lamali, A., Ayache, M., 2014. The Paleoproterozoic Djebel Drissa ring complex (Eglab shield, Algeria): post-collisional intrusions in a transtentional tectonic setting. *Tectonophysics*, 629, 197-210.

Merabet, N.E., Mahdjoub, Y., Henry, B., Abtout, A., Maouche, S., Kahoui, M., Lamali, A., Ayache, M., 2016. Paleoproterozoic structural frame of the Yetti domain (Eglab Shield, Algeria): emplacement conditions of the Tinguicht late pluton from magnetic fabric study. *Journal of African Earth Sciences*, 114, 158-173.

Merabet N.E., B. Henry, S. Maouche, A. Abou, Y. Mahdjoub, A. Lamali, M. Ayache, 2020. Paleoproterozoic structural evolution of the Eglab domain (Eglab shield, Algeria) from aeromagnetic data and anisotropy of magnetic susceptibility (AMS) study of the post-collisional Aftout granitoids. *Journal of African Earth Sciences*, 172, 103979.

Metelka, V., Baratoux, L., Naba, S., Jessell, W.M., 2011. A geophysically constrained litho-structural analysis of the Eburnean greenstone belts and associated granitoid domains, western Burkina Faso. Precambrian Research, 190, 48–69, https://doi.org/10.1016/j.precamres.2011.08.002

Metelka, V., Baratoux, L., Jessell, M.W., Naba, S., 2015. Visible and infrared properties of weathered to unaltered rocks from Precambrian granite greenstone terrains of the West African Craton. *Journal of African Earth Sciences*, 112, 570-585. https://doi.org/10.1016/j.jafrearsci.2015.10.003

Metelka, V., Baratoux, L., Jessell, M.W., Barth, A., Ježek, J., Naba, S., 2018. Automated regolith landform mapping using airborne geophysics and remote sensing data, Burkina Faso, West Africa. Remote Sensing of Environment, 204, 964-978, https://doi.org/10.1016/j.rse.2017.08.004

Michard, A., Saddiqi, O., Chalouan, A., de Lamotte, D.F. (Eds.), 2008. Continental Evolution: The Geology of Morocco: Structure, stratigraphy and tectonics of the Africa–Atlantic–Mediterranean triple junction (116). Springer.

Milési, J.P., Feybess,e J.L., Lédru, P., Dommanget, A., Ouédraogo, M.F., Marcoux, E., Prost, A., Vinchon, C., Sylvain, J.P., Johan, V., Tégyey, M., Calvez, J.Y., Lagny, P., 1989. Les minéralisations aurifères de l'Afrique de l'Ouest, leurs relations avec l'évolution lithostructurale du protérozoïque inférieur. *Chron. Rech. Min.*, Fr. 497, 3-98.

Milési, J.P., Toteu, S.F., Deschamps, Y. , Lerouge, C., Cocherie, A., Penaye, J., Tchameni, R., Moloto-A-Kenguemba, G., Kampunzu, H.A.B., Nicol, N., Duguey, E., Leistel, J.M., Saint-Martin, M., Ralay, F., Heinry, C., Bouchot, V., Doumnang Mbaigane, J.C., Kanda Kula, V., Chene, F., Monthel, J., Boutin, P., Cailteux, J., 2006. An overview of the geology and major ore deposits of Central Africa: explanatory note for the 1:4,000,000 map ''Geology and major ore deposits of Central Africa. *Journal of African Earth Sciences*, 44, 571-595., https://doi.org/10.1016/j.jafrearsci.2005.10.016

Mickus, K., 2008. Regional gravity analysis of Burkina Faso: implications for the location of metallic ore deposits. *Journal of African Earth Sciences*, 50, 55-66.

Mignon, R., 1970. Etude géologique et prospection du Damagaram Mounio et du Sud Maradi. *Rapport BRGM*, 70, 46–51, 54.

Miningou, M.Y.W., Affaton, P., Bamba, O. and Lompo, M. 2010. Mise en évidence d'une triade glaciaire néoprotérozoïque et d'une molasse dans la région du Béli, bassin du Gourma, Nord-Est Burkina Faso. *Journal of Science*, 10, 55–68.

Miningou, M.Y.W., Affaton, P., Meunier, J.D., Blot, A. and Nebie, A.G. 2017. Establishment of a lithostratigraphic column in the Béli area (Northeastern Burkina Faso, West Africa) based on the occurrence of a glacial triad and a molassic sequences in Neoproterozoic sedimentary Formations. Implications for the Pan-African orogeny. *Journal of African Earth Sciences*, 131, 80–97, https://doi.org/10.1016/j.jafrearsci.2017.03.016

Moreno, C., Sáez,, R., González, F., Almodóvar, G., Toscano, M., Playford, G., Alansari, A., Rziki, S., Bajddi, A., 2008. Age and depositional environment of the Draa Sfar massive sulfide deposit, Morocco. *Mineralium Deposita*, 43(8), 891-911.

Mortimer, J., 1990. Evolution of Early Proterozoïc Toumodi Volcanic Group and Associated Rocks, Ivory coast. *PhD thesis*, Portsmouth Polytechnic, Portsmouth, UK.

Moussine-Pouchkine, A. and Bertrand-Sarfati, J. 1978. Le Gourma: un aulacogène du Précambrien supérieur? Bull.Soc. Géol. Fr, 7 XX , 851–857, https://doi.org/10.2113/gssgfbull.S7-XX.6.851

Nahon, D., 1991. Introduction to the Petrology of Soils and Chemical Weathering. *Wiley Interscience.*

Naldrett, A.J., 2004. Magmatic sulfide deposits: Geology, Geochemistry and Exploration. *Springer Verlaag*, 728 p.

Ngako, V., Affaton, P., Nnange, J.M. and Njanko, T. 2003. Pan-African tectonic evolution in central and southern Cameroon: transpression and transtension during sinistral shear movements. *Journal of African Earth Sciences*, 36, 207–214, https://doi.org/10.1016/S0899-5362(03)00023-X

Ngako, V., Affaton, P., Njonfang, E., 2008. Pan-African tectonic in northwestern Cameroon: Implication for history of Western Gondwana. *Gondwana Research*, 14, 509-522.

Nyame, F.K., Armah, T.K.E., Ibrahim, K., Baah-Acheamfour, J., Manu, J., Tigme, J., 2020. Manganese occurrence in the Mankwadzi Area, southern Kibi-Winneba metavolcanic belt, Ghana: typical or atypical palaeoproterozoic Birimian Mn mineralization? *Geological Society, London, Special Publications*, **502**, https://doi.org/10.1144/SP502-2019-75

Njonfang, E., Ngako, V., Moreau, C., Affaton, P., Diot, H., 2008. Restraining bends in high temperature shear zones: the 'Central Cameroon Shear Zone', Central Africa. *Journal of African Earth Sciences*, 52, 9–20.

Ntep, G.P. 1993. Carte de l'Or et du diamant de la province de l'Est Cameroun. Artisanaux des substances précieuses, à l'échelle de 1/500000. DMG/MINMEE, Yaoundé, Cameroun.

Ntep, G.P. 1994. Point sur l'exploitation artisanale des substances précieuses dans la province de l'Est-Cameroun.

Ntep, G.P., Dupuy, J., Matip, O., Fogakoh, F.A. and Kalngui, E., 2001. Notice explicative de la carte thématique des ressources minérales du Cameroun.

Oberthür, T., Melcher, F., Henjes-Kunst, F., Gerdes, A., Stein, H., Zimmerman, A., El Ghorfi, M., 2009. Hercynian age of the cobalt-nickel-arsenide-(gold) ores, Bou Azzer, Anti-Atlas, Morocco: Re-Os, Sm-Nd, and U-Pb age determinations. *Economic Geology*, 104, 1065–1079, https://doi.org/10.2113/econgeo.104.7.1065

Ogezi, A.E.O. 1977. Geochemistry and Geochronology of Basement Rocks from North Western Nigeria. *PhD thesis*, Leeds University, Leeds, UK.

Okubo, Y., Graf, R.J., Hansen, R.O., Ogawa, K., Tsu, H,. 1985. Curie point depths of the island of Kyushu and surrounding areas, Japan. *Geophysics*, 50, 481–494, https://doi.org/10.1190/1.1441926

Onstott, T.C., Dorbor, J. 1987. $^{40}Ar/^{39}Ar$ and paleomagnetic results from Liberia and the Precambrian APW database for the West African Shield. Journal of African Earth Sciences, 6, 537–552, https://doi.org/10.1016/0899-5362(87)90094-7

Onstott, T.C., Hargraves, R.B., York, D., Hall, C. 1984. Constraints on the motions of South American and African shields during the Proterozoic: I. $^{40}Ar/^{39}Ar$ and paleomagnetic correlations between Venezuela and Liberia. *Geological Society of America Bulletin*, 95, 1045–1054, https://doi.org/10.1130/0016-7606 (1984) 95, 1045: COTMOS.2.0.CO;2

Omang, B., Bih, C., Fon, A., Embui, V., Suh, C.E., 2014. Regional geochemical stream sediment survey for gold exploration in the upper Lom basin, Eastern Cameroon. *International Journal of Geosciences*, 5, 1012–1026, https://doi.org/10.4236/ijg.2014.59087

Omang, B.O., Suh, C.E. et al., 2015. Microchemical signature of alluvial gold from two contrasting terrainsin Cameroon. *Journal of African Earth Sciences*, 112, 1–14, https://doi.org/10.1016/j.jafrearsci.2015.09.004

Ouattara, N., 1998. Pétrologie, géochimie et métallogénie des sulfures et des éléments du groupe du platine des ultrabasites de Côte d'Ivoire: Signification géodynamique et implications sur les processus de croissance crustale à l'Archéen et au Paléoprotérozoïque. *Thèse de doctorat*, Université d'Orléans, France.

Ouattara, Z., 2015. Caractères lithostratigraphique, structural, géochimique et métallogénique du gisement d'or de Bonikro, sillon birimien de Fèttékro, centre-sud de la Côte d'Ivoire. *PhD Thesis*, Université Félix Houphouët-Boigny, Abidjan, Côte d'Ivoire.

Ouattara, Z., Coulibaly, Y., Lieben, F., 2015. Pétrographie du gisement d'or de Bonikro, sillon birimien d'Oumé-Féttèkro, Côte d'Ivoire. *European Scientific Journal*, 11, 119–132.

Ouattara, A.S., Coulibaly, Y. and Kouadio, F.J.L.H. 2017. Les altérations hydrothermales associées à la minéralisation aurifère du gisement de Dougbafla (district d'Oumé-Hiré, centre-ouest de la Côte d'Ivoire). *European Scientific Journal*, 13, 108–125, https://doi.org/10.19044/esj.2017.v13n30p108

Ouattara, Z., Coulibaly, Y. and Boiron, M.C. 2018a. Lithostratigraphy of the Bonikro gold deposit: contribution to the setting of the Birimian units in the southern Fettèkro greenstone belt, Cote d'Ivoire. *Revue Sciences de la vie, de la Terre et Agronomie*, 6, 6–14.

Ouattara, Z., Coulibaly, Y. and Boiron, M.C. 2018b. Apport des minéraux d'altération dans la caractérisation du gisement d'or de Bonikro, sillon birimien de Fettèkro, Côte d'Ivoire. *Afrique Science*, 14, 343–358.

Ouattara, Z., Coulibaly, Y., Boiron, M.C., 2020. Shear-hosted gold mineralization in the Oumé-Fettèkro greenstone belt, Côte d'Ivoire: the Bonikro deposit. *Geological Society, London, Special Publications*, **502**, https://doi.org/10.1144/SP502-2019-103

Outigua, A., Essaifi, A., Corsini, M., Outhounjite, M., Zouhair, M., 2020. Sidi M'Barek: a representative example of the Moroccan massive sulfide deposits. *Geological Society, London, Special Publications*, **502**, https://doi.org/10.1144/SP502-2019-65

Pesonen, L.J., Bylund, G., Torsvik, T.H., Elming, S.A., Mertanen, S., 1991. Catalogue of palaeomagnetic directions and poles from Fennoscandia: Archaen to Tertiary. *Tectonophysics*, 195, 151–207, https://doi.org/10.1016/0040-1951(91)90210-J

Peucat, J.J., Capdevila, R., Drareni, A., Mahdjoub, Y., Kahoui, M., 2005. The Eglab massif in the West African Craton (Algeria), an original segment of the Eburnean orogenic belt: petrology, geochemistry and geochronology. *Precambrian Research*, 136, 309–352, https://doi.org/10.1016/j.precamres.2004.12.002

Pokorny, B., von Lübke, C., Dayamba, S.D., Dickow, H., 2019. All the gold for nothing? Impacts of mining on rural livelihoods in Northern Burkina Faso. *World Development*, 119, 23-39, https://doi.org/10.1016/j.worlddev.2019.03.003

PRDSM. 2005. Projet de géophysique aéroportée dans le secteur Sud Maradi. *Ministère des Mines et de développement Industriel, Programme for the Strengthening and Diversification of the Mining Sector* (PRDSM).

Roberts, M.P., Clemens, J.D., 1993. Origin of high-potassium, calc-alkaline, I-type granitoids. *Geology*, 21, 825-828.

Rogers, J.J.W., Santosh, M., 2002a. Configuration of Columbia, a Mesoproterozoic supercontinent. *Gondwana Research*, 5(1), 5–22, https://doi.org/10.1016/S1342-937X(05)70883-2

Rogers, J.J.W., Santosh, M. (eds), 2002b. Mesoproterozic supercontinent. *Gondwana Research*, 5(1), 3–255.

Rogers, J.J.W. and Santosh, M. 2003. Supercontinents in Earth history. *Gondwana Research*, 6, 357–368, https://doi.org/10.1016/S1342-937X(05)70993-X

Rogers, J.J.W., Santosh, M., 2004. Continents and Supercontinents. *Oxford University Press*, New York, 298.

Rziki, S., 2012. Le gisement polymétallique de Draa Sfar: compilation et modélisation tridimentionnelle, géologique, géophysique et perspectives de développement (Massif Hercynien des Jebilet Centrales, Maroc). *PhD thesis*, Marrakech University, Morocco.

Rziki, S., Alansari, A., Mouguina, E.M., Simard, J., Zouhair, M., Maacha, L., 2012. Apport du modèle géologique et géophysique 3D dans le développement du gisement polymétallique de Draa Sfar (Massif hercynien des Jebilet centrales, Maroc). *Estudios Geológicos*, 68(1), 29-40. https://doi.org/10.3989/egeol.40366.138

Sabaté, P., 1978. Données géochimiques et radiométriques sur les volcanites calcoalcalines précambriennes de l'Eglab (Sahara occidental algérien). Esquisse de leur évolution géotectonique. *Bulletin de la Société Géologique de France*, 7, XX(1), 81–90, https://doi.org/10.2113/gssgfbull.S7-XX.1.81

Sabaté, P., 1979. Les volcanites Eglab: données radiométriques de la dernière expression magmatique calcoalcaline du cycle orogénique Eglab (Sahara occidental). *Revue de Géologie Dynanique et de Géographie Physique*, 21, 326–329.

Sabaté, P., Lomax, K., 1975. Données stratigraphiques et paléomagnétiques de la région Yetti–Eglab (Sahara occidental algérien). *Bulletin du BRGM* (deuxième série), section II, 4, 293–311.

Sabaté, P., Lameyre, J., 1973. Magmatism and metamorphism in the Yetti–Eglab Precambrian formations of the R'guibat dorsale (Occidental Algerian Sahara). *7th Colloquium on the Geology of Africa, Florence, Italy and Travaux des Laboratoires des Sciences de la Terre*, Marseille, B, 11, 131–133, Abstracts.

Saddiqi, O., I. Manighetti, A. Michard (Eds.), 2018. The West African Craton and its margins. A tribute to Professor André Michard for his jubilee of works in Morocco. *Comptes Renndus Geoscience*, 350, 6, 231-330.

Sangster, D.F., 1996a. Mississippi Valley-type lead-zinc, *in* Eckstrand, O.R., Sinclair, W.D., Thorpe, R.I., eds., Geology of Canadian mineral deposit types. *Geological Survey of Canada*, Geology of Canada, 8, 253–261.

Sangster, D.F. (Ed.), 1996b. Carbonate hosted lead-zinc deposits. *Society of Economic Geologist Special Publication* Number 4, 664 p.

Saquaque, A., Benharref, M., Abia, H., Mrini, Z., Reuber, I., Karson, J.A., 1992. Evidence for a Panafrican volcanic arc and wrench fault tectonics in the Jbel Saghro, Anti-Atlas, Morocco. *Geologische Rundschau*, 81, 1–13, https://doi.org/10.1007/BF01764536

Scholten, L., Watenphul, A., Beermann, O., Testemale, D., Ames, D., Schmidt, C., 2018. Nickel and platinum in high-temperature H2O + HCl fluids: implications for hydrothermal mobilization. *Geochimica Cosmochimica Acta*, 224, 187–199, https://doi.org/10.1016/j.gca.2018.01.005

Shoji, S., Dahlgren, R., Nanzyo, M., 1993. Morphology of volcanic ash soils. *Developments in Soil Scienc*e, 21, 7–3, https://doi.org/10.1016/S0166-2481(08)70263-0

Siagné Z.H., T. Aïfa, A.N. Kouamelan, N.N. Houssou, W. Digbeu, B.K.F. Kakou, P. Couderc, 2021. New lithostructural map of the Doropo region, N-E Côte d'Ivoire: Contribution of aeromagnetic and structural data. *Journal of African Earth Sciences*, moderate revision, revised.

Singer, D.A., Berger, V.I., Moring, B.C., 2002. Porphyry copper deposits of the world: database, maps, and preliminary analysis: *U.S. Geological Survey Open–File Report 02–268*, available online at http://geopubs.wr.usgs.gov/open-file/of02-268/

Soba, D., Michard, A. et al., 1991. Données Géochronologiques nouvelles (Rb–Sr, U–Pb et Sm–Nd) sur la zone mobile panafricaine de l'Est-Cameroun: âge protérozoïque supérieur de la serie de Lom. *Comptes Rendus Academie Sciences Paris*, 312, 1453–1458.

Soulaimani, S., Chakiri, S., Manar, A., Soulaimani, A., Miftah, A., Boujamaoui, M., 2020. Gravity and magnetic data processing further constrained inversion for 3D modelling and tonnage calculation. *Applied Earth Science*, https://doi.org/10.1080/25726838.2020.1767473

Soumaïla, A., Henry, P., Garba, Z., Rossi, M., 2008. REE Patterns, Nd-Sm and U-Pb ages of the metamorphic rocks of the Diagorou-Darbani greenstone belt (Liptako, SW Niger): implication for Birimian (Paleoproterozoic) crustal genesis. *Geological Society*, London, Special Publications, 297, 19-32, https://doi.org/10.1144/SP297.2

Suh, C.E., Lehmann, B., Mafany, G.T., 2006. Geology and geochemical aspects of lode gold mineralization at Dimako–Mboscorro, SE Cameroon. *Geochemistry Exploration, Environment, Analysis*, 6, 295–309, https://doi.org/10.1144/1467-7873/06-110

Stern, R.J., 1994. Arc assembly and continental collision in the Neoproterozoic East African orogeny – implications for the consolidation of Gondwana. Annual Review of Earth and Planetary Sciences, 22, 319–351, https://doi.org/10.1146/annurev.ea.22.050194.001535

Tanaka, A., Okubo, Y., Matsubayashi, O., 1999. Curie point depth based on spectrum analysis of the magnetic anomaly data in East and Southeast Asia. *Tectonophysics*, 306, 461–470, https://doi.org/10.1016/S0040-1951(99)00072-4

Taylor, C.D., Schulz, K.J., Doebrich, J.L., Orris, G.J., Denning, P.D., and Kirschbaum, M.J., 2009, Geology and nonfuel mineral deposits of Africa and the Middle East: *U.S. Geological Survey Open-File Report 2005*–1294-E, 246p.

Taylor, C.D., Bradley, D.C., Finn, C.A., Zerrouki, A., Ayad, B., Belanteur, N.F., Bouchilaoune, N., Johnson, M.R., Meziane, G., Mihalasky, M.J., Mouchene, H., Oughou, S., Smith, S.M., Solano, F., Zerrouk , S., 2019. Metallogenic implications of a new geodynamic model for the Eglab, Algeria. *4th IGCP638 Meeting*, 28 October to 2 November, Algiers, 3.

Tchaptchet, T.W., Tematio, P., Guimapi, T.N., Happi, E., Tiomo, I., Momo, N.M., 2020. Morphological, mineral and geochemical characterization of soil profiles in Meïganga as tools for rock weathering intensity and trend evaluation and residual ore deposit prospection in the mineralized domain of central Cameroon. *Geological Society, London, Special Publications*, **502**, https://doi.org/10.1144/SP502-2019-84

Tchaptchet Tchato, D., Schulz, B., Nzenti, J.P., 2009. Electron microprobe dating and thermobarometry of Neoproterozoic metamorphic events in the Kékem area, Central African Fold Belt of Cameroon. Neues Jahrbuch für Mineralogie-Abhandlungen, 186(1), 95-109, https://doi.org/10.1127/0077-7757/2009/0140

Tcheumenak Kouémo, J., Njanko, T., Kwékam, M., Naba, S., Bella Nké, B.E., Yankeu Sandjo, A.F., Fozing, E., Njonfang, E., 2014. Kinematic evolution of the Fodjomekwet-Fotouni Shear Zone (West-Cameroon): implication on the emplacement of the Fomopéa and Bandja plutonic massifs: Journal of African Earth Sciences 99, 261-275.

Tewari, V.C., Seckbach, J. (eds)., 2011. Stromatolites: Interaction of Microbes with Sediments. Cellular Origin, Life in Extreme Habitats and Astrobiology. *Springer*, *Dordrecht*, 751, https://doi.org/10.1007/978-94-007-0397-1

Toteu, S.F., Yongue Fouateu, R. et al. 2006. U–Pb dating of plutonic rocks involved in the nappe tectonic in Southern Cameroon: consequence for the Pan-African orogenic evolution of the central African fold belt. *Journal of African Earth Sciences*, 44, 479–493.

Tshibubudze, A., Hein, K.A.A. 2013. Structural setting of gold deposits in the Oudalan-Gorouol volcano-sedimentary belt east of the Markoye Shear Zone, West African Craton. *Journal of African Earth Sciences*, 80, 31-47, https://doi.org/10.1016/j.jafrearsci.2012.11.010

Trompette, R., 1997. Neoproterozoic (c. 600 Ma) aggregation of Western Gondwana: a tentative scenario. *Precambrian Research*, 82, 101–112, https://doi.org/10.1016/S0301-9268(96)00045-9

Van Breemen, O., Pidgeon, R.T., Bowden, P., 1977. Age and isotopic studies of some Pan-African granites from north-central Nigeria. *Precambrian Research*, 4, 307–319, https://doi.org/10.1016/0301-9268(77)90001-8

Van Hinsbergen, D.J.J., Buiter, S.J.H., Torsvik, T.H., Gaina, C., Webb, S.J. (eds), 2011. The Formation and Evolution of Africa: A Synopsis of 3.8 Ga of Earth History. *Geological Societ*y, London, Special Publications, 357, 1-8, https://doi.org/10.1144/SP357.1

Villeneuve, M., Cornée, J.J. 1994. Structure, evolution and palaeogeography of West African craton and bordering belts during the Neoproterozoic. *Precambrian Research*, 69, 307–326, https://doi.org/10.1016/0301-9268(94)90094-9

Vishiti, A., Suh, C.E., Lehmann, B., Egbe, J.A., Schemang, E.M., 2015. Gold grade variation and particle microchemistry in exploration pits of the Batouri gold district, SE Cameroon. *Journal of African Earth Sciences*, 111, 1–13, https://doi.org/10.1016/j.jafrearsci.2015.07.010

Vishiti, A., Suh, C.E., et al., 2017. Mineral chemistry, bulk rock geochemistry, and S-isotopesignature of lode-gold mineralization in the Bétaré–Oyagolddistrict, southeast Cameroon. *Geological Journal*, 2017, 1–18.

Walid, M.A., Susilo, A., Sunaryo, 2013. Mapping of manganese ore deposits by using geomagnetic method in Aceh Jaya District, Nangro Aceh Darussalam Province. Indonesia. International Refereed Journal of Engineering and Science (IRJES), 10, 12–20.

Weber, A.P., Roberts, S., Taylor, R.N., Pitcairn, K., 2012. Golden plumes: substantial gold enrichment of oceanic crust during ridge–plume interaction. *Geology*, 41, 87–90, https://doi.org/10.1130/G33301.1

Wilburn, D.R., 2004, Nonfuel mineral exploration 2003. *Mining Engineering*, 56, 25–37.

Wilkin, R.T., Bornhorst, T.J., 1992. Geology and geochemistry of granitoid rocks in the Archean Northern Complex, Michigan, USA. *Canadian Journal of Earth Sciences*, 29, 1674-1685, htttps://doi.org/10.1139/e92-132

Williams, I.S., Claesson, S., 1987. Isotopic evidence for the Precambrian provenance and Caledonian metamorphism of high grade paragneiss from the Seve Nappes, Scandinavian Caledonides. *Contributions to Mineralogy and Petrology*, 97, 205–217, https://doi.org/10.1007/BF00371240

Yacé, I. ,1982. Etude géologique du volcanisme éburnéen dans les parties centrale et méridionale de la chaîne précambrienne de Fettèkro. *Ministère des Mines et de la Géologie*, Abidjan, Côte d'Ivoire.

Yousefi M., V.Nykänen (Eds.), 2017. GIS-based mineral potential targeting. *Journal of African Earth Sciences*, 128, 1-176.

Zaw, K., Peters, S.G., Cook, N.J., Hou, Z. (Eds.), 2007. Mineral deposits of South China. *Ore Geology Reviews*, 31, 1-384.

Zeng, Z., Cui, Y.J., Zhang, F., Conil, N., Talandier, J., 2019. Investigation of swelling pressure of bentonite/claystone mixture in the full range of bentonite fraction. *Applied Clay Science*, 178, 1–7, https://doi.org/10.1016/j.clay.2019.105137

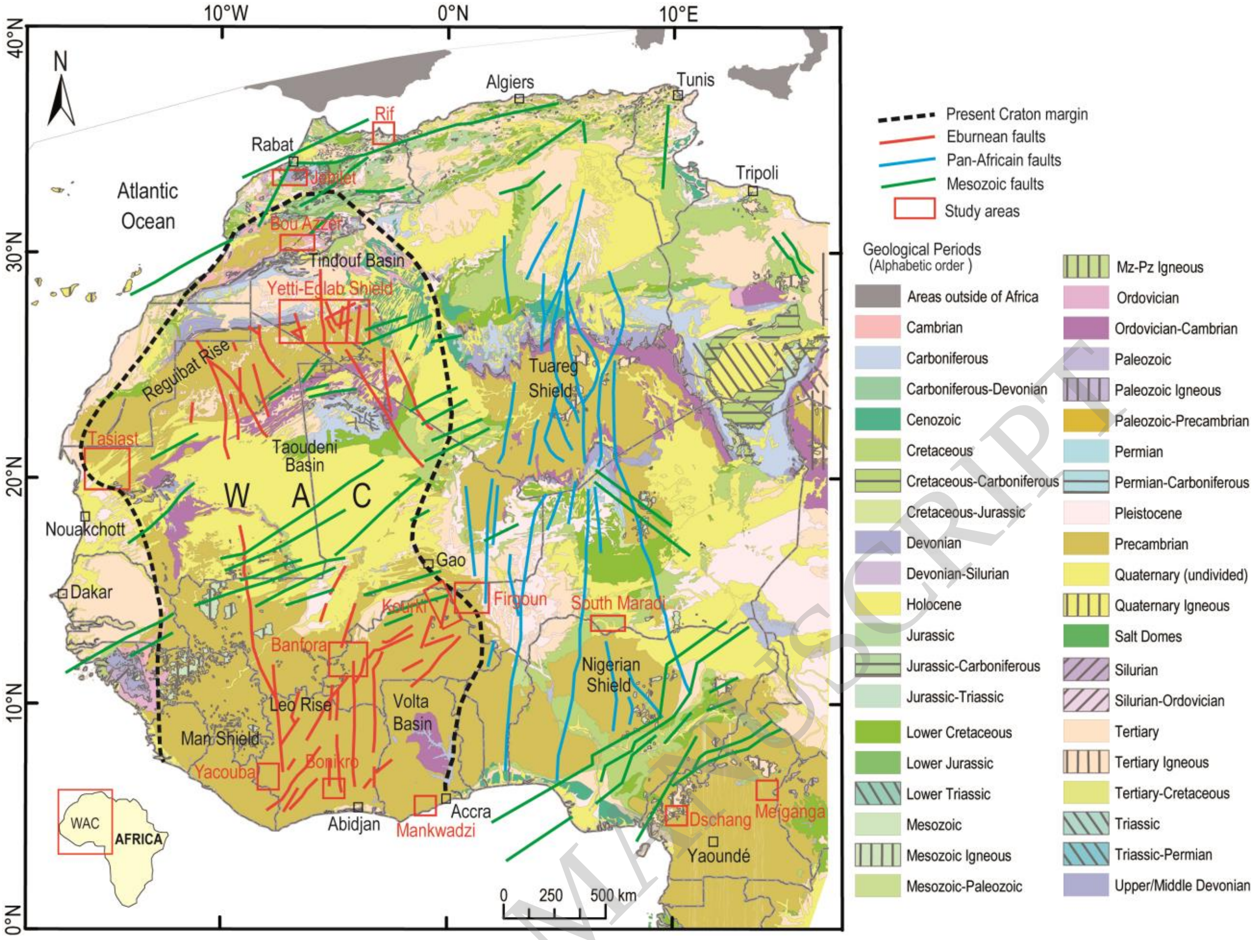

10°W
0°N
10°E
40°N
30°N
20°N
10°N
0°N
N
Atlantic Ocean
Rabat
Algiers
Tunis
Tripoli
Rif
Tindouf Basin
Yetti-Eglab Shield
Reguibat Rise
Tasiast
Taoudeni Basin
W A C
Nouakchott
Dakar
Gao
Tuareg Shield
Kourki
Firgoun
South Maradi
Bantora
Nigerian Shield
Leo Rise
Volta Basin
Man Shield
Yacouba
Bonikro
Abidjan
Accra
Mankwadzi
Dschang
Meiganga
Yaoundé
WAC
AFRICA
0 250 500 km
Present Craton margin
Eburnean faults
Pan-Africain faults
Mesozoic faults
Study areas
Geological Periods (Alphabetic order)
Areas outside of Africa
Cambrian
Carboniferous
Carboniferous-Devonian
Cenozoic
Cretaceous
Cretaceous-Carboniferous
Cretaceous-Jurassic
Devonian
Devonian-Silurian
Holocene
Jurassic
Jurassic-Carboniferous
Jurassic-Triassic
Lower Cretaceous
Lower Jurassic
Lower Triassic
Mesozoic
Mesozoic Igneous
Mesozoic-Paleozoic
Mz-Pz Igneous
Ordovician
Ordovician-Cambrian
Paleozoic
Paleozoic Igneous
Paleozoic-Precambrian
Permian
Permian-Carboniferous
Pleistocene
Precambrian
Quaternary (undivided)
Quaternary Igneous
Salt Domes
Silurian
Silurian-Ordovician
Tertiary
Tertiary Igneous
Tertiary-Cretaceous
Triassic
Triassic-Permian
Upper/Middle Devonian

Figure 1a

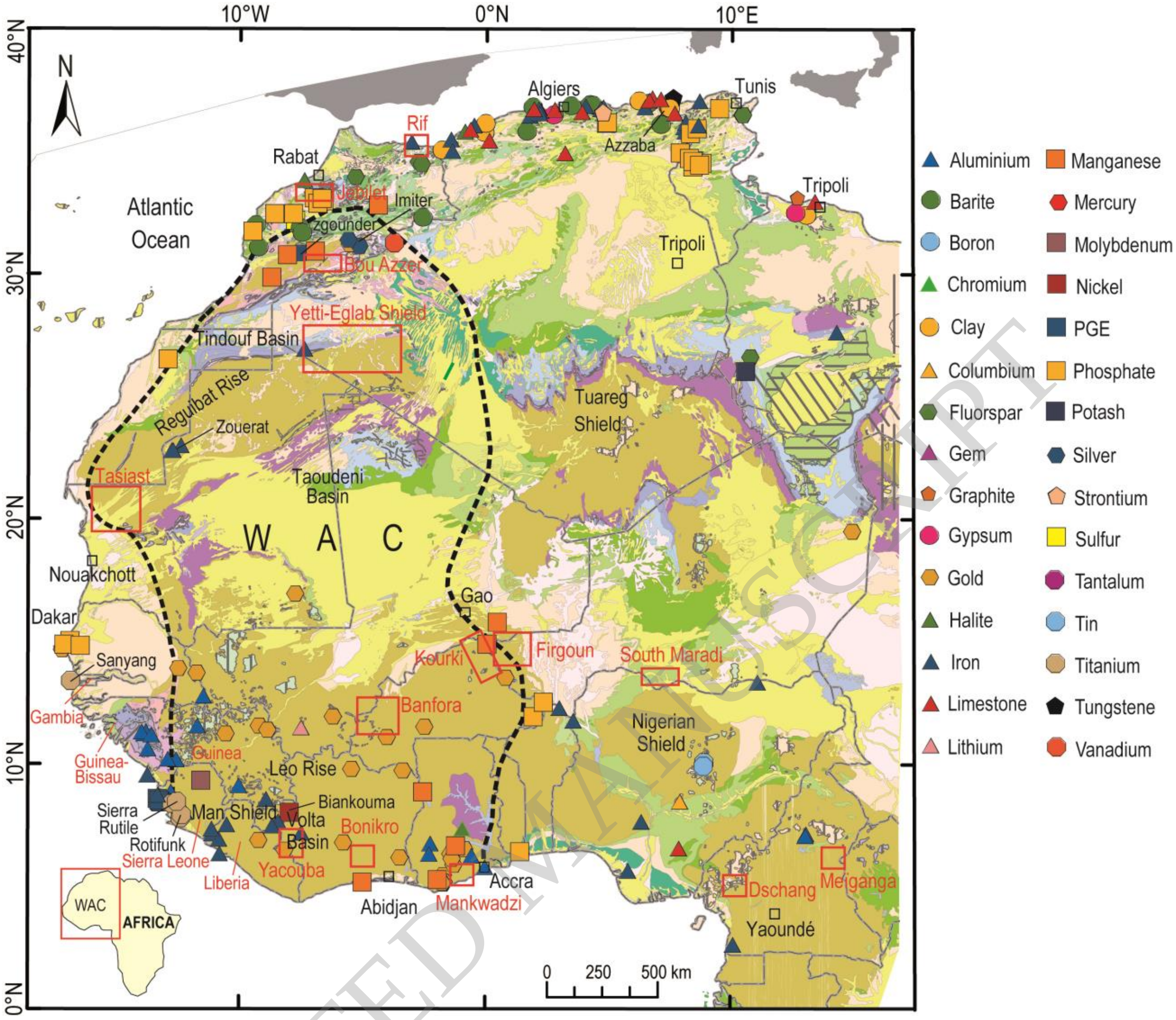

10°W
0°N
10°E
40°N
30°N
20°N
10°N
0°N
N
Atlantic Ocean
Algiers
Tunis
Rif
Azzaba
Rabat
Tripoli
Jebilet
Imiter
Zgounder
Bou Azzer
Tripoli
Yetti-Eglab Shield
Tindouf Basin
Reguibat Rise
Zouerat
Tuareg Shield
Tasiast
Taoudeni Basin
W A C
Nouakchott
Dakar
Gao
Sanyang
Kourki
Firgoun
South Maradi
Gambia
Banfora
Guinea-Bissau
Guinea
Leo Rise
Nigerian Shield
Sierra Rutile
Man Shield
Biankouma
Volta Basin
Bonikro
Rotifunk
Sierra Leone
Liberia
Yacouba
Accra
Abidjan
Mankwadzi
Dschang
Meiganga
Yaoundé
WAC
AFRICA
0 250 500 km
Aluminium
Barite
Boron
Chromium
Clay
Columbium
Fluorspar
Gem
Graphite
Gypsum
Gold
Halite
Iron
Limestone
Lithium
Manganese
Mercury
Molybdenum
Nickel
PGE
Phosphate
Potash
Silver
Strontium
Sulfur
Tantalum
Tin
Titanium
Tungstene
Vanadium

Figure 1b

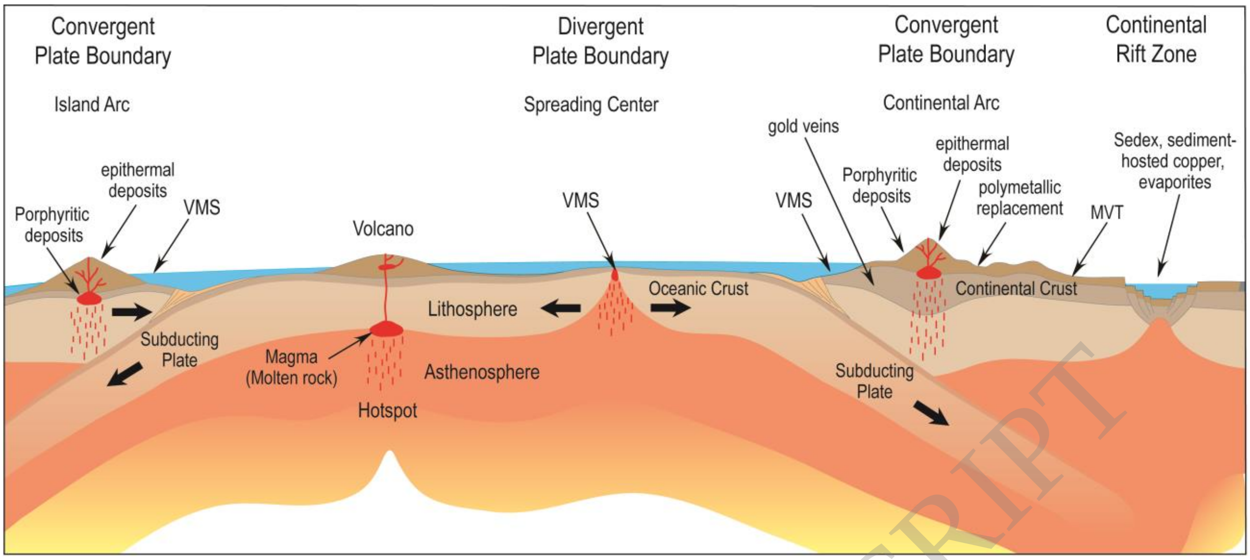
Convergent
Plate Boundary
Island Arc
epithermal
deposits
Porphyritic
deposits
VMS
Subducting
Plate
Volcano
Magma
(Molten rock)
Hotspot
Lithosphere
Asthenosphere
Divergent
Plate Boundary
Spreading Center
VMS
Oceanic Crust
Convergent
Plate Boundary
Continental Arc
gold veins
VMS
Porphyritic
deposits
epithermal
deposits
polymetallic
replacement
Continental Crust
Subducting
Plate
Continental
Rift Zone
Sedex, sediment-
hosted copper,
evaporites
MVT

Figure 2

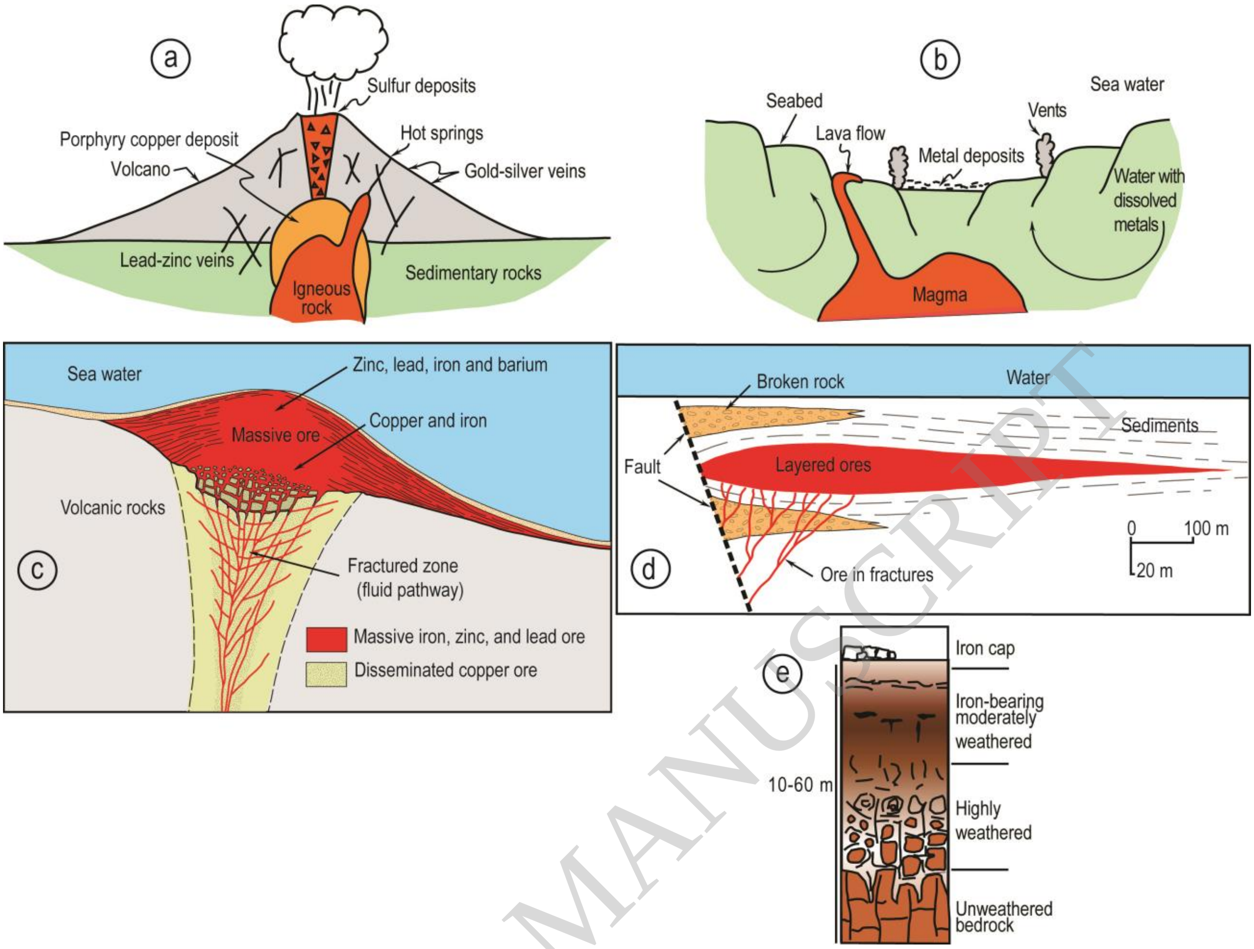
a
Sulfur deposits
Porphyry copper deposit
Hot springs
Volcano
Gold-silver veins
Lead-zinc veins
Sedimentary rocks
Igneous rock
b
Sea water
Seabed
Vents
Lava flow
Metal deposits
Water with dissolved metals
Magma
Sea water
Zinc, lead, iron and barium
Copper and iron
Massive ore
Volcanic rocks
c
Fractured zone (fluid pathway)
Massive iron, zinc, and lead ore
Disseminated copper ore
Broken rock
Water
Sediments
Fault
Layered ores
0
100 m
20 m
d
Ore in fractures
e
Iron cap
Iron-bearing moderately weathered
10-60 m
Highly weathered
Unweathered bedrock

Figure 3